

ALK1 (Activin-Receptor Like Kinase 1) Loss Results in Vascular Hyperplasia in Mice and Humans Through PI3K (Phosphatidylinositol 3-Kinase) Activation

Elisenda Alsina-Sanchís,* Yaiza García-Ibáñez,* Ana M. Figueiredo, Carla Riera-Domingo, Agnès Figueras, Xavier Matias-Guiu, Oriol Casanovas, Luisa M. Botella, Miquel A. Pujana, Antoni Riera-Mestre, Mariona Graupera,† Francesc Viñals†

Objective—ALK1 (activin-receptor like kinase 1) is an endothelial cell-restricted receptor with high affinity for BMP (bone morphogenetic protein) 9 TGF- β (transforming growth factor- β) family member. Loss-of-function mutations in ALK1 cause a subtype of hereditary hemorrhagic telangiectasia—a rare disease characterized by vasculature malformations. Therapeutic strategies are aimed at reducing potential complications because of vascular malformations, but currently, there is no curative treatment for hereditary hemorrhagic telangiectasia.

Approach and Results—In this work, we report that a reduction in ALK1 gene dosage (heterozygous ALK1^{+/-} mice) results in enhanced retinal endothelial cell proliferation and vascular hyperplasia at the sprouting front. We found that BMP9/ALK1 represses VEGF (vascular endothelial growth factor)-mediated PI3K (phosphatidylinositol 3-kinase) by promoting the activity of the PTEN (phosphatase and tensin homolog). Consequently, loss of ALK1 function in endothelial cells results in increased activity of the PI3K pathway. These results were confirmed in cutaneous telangiectasia biopsies of patients with hereditary hemorrhagic telangiectasia 2, in which we also detected an increase in endothelial cell proliferation linked to an increase on the PI3K pathway. In mice, genetic and pharmacological inhibition of PI3K is sufficient to abolish the vascular hyperplasia of ALK1^{+/-} retinas and in turn normalize the vasculature.

Conclusions—Overall, our results indicate that the BMP9/ALK1 hub critically mediates vascular quiescence by limiting PI3K signaling and suggest that PI3K inhibitors could be used as novel therapeutic agents to treat hereditary hemorrhagic telangiectasia. (*Arterioscler Thromb Vasc Biol.* 2018;38:00-00, DOI: 10.1161/ATVBAHA.118.310760.)

Key Words: animals ■ humans ■ mice ■ rare diseases ■ retina

Blood vessels play essential roles in the transport of gases, nutrients, waste products, and circulating cells in the healthy organism. Although vessels are quiescent in adults, the growth of blood vessels is critical to development, growth, and regeneration.^{1,2} Angiogenesis—the formation of new blood vessels—consists of sprouting new vessels from preexisting ones and the eventual fusion of these with other sprouts or blood vessels to form new vascular connections. Vessel growth is stimulated by angiogenic factors, which are divided into (1) activators, such as VEGF-A (vascular endothelial growth factor-A; hereafter referred to as VEGF), FGF

(fibroblast growth factor) 2, and EGF (epidermal growth factor), which induce endothelial cell proliferation and migration^{1,3}; and (2) maturation factors, such as TNF- α (tumor necrosis factor- α), IL-8 (interleukin-8) and some members of the TGF- β (transforming growth factor- β) family, which prompt endothelial cells to cease proliferation, reestablish basal membrane, and recruit mural cells.^{4,5} BMP (bone morphogenetic protein) 9 is a member of the TGF- β family that selectively activates ALK1 (activin receptor-like kinase)—a serine-threonine kinase type I TGF- β receptor in endothelial cells.⁶ Activation of ALK1 triggers the phosphorylation of

Received on: August 31, 2017; final version accepted on: January 31, 2018.

From the Program Against Cancer Therapeutic Resistance, Institut Català d'Oncologia, Hospital Duran i Reynals (E.A.-S., Y.G.-I., A.M.F., C.R.-D., A.F., O.C., M.A.P., M.G., F.V.) and Vascular Signaling Laboratory, Institut d'Investigació Biomèdica de Bellvitge (M.G.), L'Hospitalet de Llobregat, Barcelona, Spain; Institut d'Investigació Biomèdica de Bellvitge, Spain (E.A.-S., Y.G.-I., A.M.F., C.R.-D., A.F., X.M.-G., O.C., M.A.P., F.V.); Servei d'Anatomia Patològica (X.M.-G.) and HHT Unit, Internal Medicine Department (A.R.-M.), Institut d'Investigació Biomèdica de Bellvitge, Hospital Universitari de Bellvitge, Spain; Hospital Universitari Arnau de Vilanova, Lleida, Spain (X.M.-G.); Universitat de Lleida, Spain (X.M.-G.); Centro de Investigaciones Biológicas, Consejo Superior de Investigaciones Científicas, Madrid, Spain (L.M.B.); Departament de Ciències Clíniques, Universitat de Barcelona, Spain (A.R.-M.); CIBERONC (M.G.); and Departament de Ciències Fisiològiques, Campus de Bellvitge, L'Hospitalet de Llobregat, Universitat de Barcelona, Spain (F.V.).

*These authors contributed equally to this article.

†M. Graupera and F. Viñals are joint last authors.

The online-only Data Supplement is available with this article at <http://atvb.ahajournals.org/lookup/suppl/doi:10.1161/ATVBAHA.118.310760/-/DC1>.

Correspondence to Francesc Viñals, Program Against Cancer Therapeutic Resistance, Institut Català d'Oncologia, Hospital Duran i Reynals, 08908 L'Hospitalet de Llobregat, Gran Via 199–203, Barcelona, Spain, E-mail fvinyals@iconcologia.net; or Mariona Graupera, Vascular Signaling Laboratory, Institut d'Investigació Biomèdica de Bellvitge, Hospital Duran i Reynals, 08908 L'Hospitalet de Llobregat, Gran Via 199–203, Barcelona, Spain, E-mail mgraupera@idibell.cat

© 2018 American Heart Association, Inc.

Arterioscler Thromb Vasc Biol is available at <http://atvb.ahajournals.org>

DOI: 10.1161/ATVBAHA.118.310760

Nonstandard Abbreviations and Acronyms

ALK1	activin receptor-like kinase 1
AVM	arteriovenous malformation
BMP	bone morphogenetic protein
EGF	epidermal growth factor
ERK	extracellular signal-regulated kinase
FGF	fibroblast growth factor
HHT	hereditary hemorrhagic telangiectasia
HUVEC	human umbilical vein endothelial cell
IB4	isolectin B4
ID1	inhibitor of differentiation 1
IL-8	interleukin-8
PI3K	phosphatidylinositol 3-kinase
PTEN	phosphatase and tensin homolog
RT	room temperature
TGF-β	transforming growth factor- β
TNF-α	tumor necrosis factor- α
VEGF	vascular endothelial growth factor

Smad1, 5, and 8, which in turn forms an active complex with Smad4, translocates to the nucleus, and stimulates the expression of genes, such as *ID*, *endoglin*, and *Tmem100*.⁷⁻⁹ BMP9 has been proposed as limiting VEGF- and FGF-induced endothelial cell proliferation.^{6,10,11} However, it is still unclear how ALK1 negatively regulates proangiogenic cascades. Given the inhibitory role of ALK1 during vessel growth, it is not surprising that genetic and pharmacological blockage of ALK1 in vivo results in aberrant overgrowth of the vasculature.^{12,13}

Hereditary hemorrhagic telangiectasia (HHT), also known as Rendu–Osler–Weber syndrome, is a rare autosomal-dominant germline disease, with an incidence of 1:5000, characterized by the local overgrowth of the vascular plexus.¹⁴ The telangiectasia is the common name for vascular lesions in patients with HHT¹⁵ and consists of an artery directly connected to a vein that generates a fragile site that can easily rupture and bleed. The telangiectasias are found on the skin of the face and hands and the lining of the nose and mouth. Less common, but more severe, are the internal vascular lesions, which principally occur in lung, liver, and the digestive tract and may lead to hemorrhagic episodes, stroke, or brain abscesses secondary to pulmonary arteriovenous malformations (AVMs), or arterial aneurysms and pulmonary arterial hypertension, or high-output heart failure secondary to liver vascular malformations.¹⁶ HHT is divided into HHT types 1 and 2 on the basis of the mutation responsible for the pathogenesis of the disease. Although HHT1 arises from inactivation mutations in *ENG*, the gene encoding the TGF- β coreceptor endoglin¹⁷ HHT2 is caused by mutations in *ACVRL1*—the gene encoding ALK1.¹⁸ Pulmonary and cerebral AVMs are more common in HHT1, whereas hepatic vascular malformations predominate in HHT2. Therapeutic strategies are aimed at reducing potential complications because of vascular malformations, but there is currently no curative treatment for HHT.

In this study, we used heterozygous *ALK1* mouse retinas and cultured endothelial cells to study how ALK1 represses vessel growth. We found that loss of ALK1 leads to increased

stalk cell proliferation as a result of overactivation of PI3K (phosphatidylinositol 3-kinase) signaling. By analyzing a small cohort of patients, we found that mutations in ALK1 result in increased activation of PI3K signaling in human telangiectasias compared with control vessels. These findings, together with the observation that blocking the PI3K signaling pathway rescues ALK1-induced vascular hyperplasia, provide the proof of concept for therapeutic intervention with PI3K inhibitors for the treatment of HHT.

Materials and Methods

Reagents

BMP9 was obtained from Sigma-Aldrich (St. Louis, MO). VEGF was obtained from R&D Systems (Minneapolis, MN). LDN-212854 was obtained from Selleckchem.com (Houston, TX) and was dissolved in DMSO. SF1670 was obtained from Echelon Biosciences (Salt Lake City, UT) and was dissolved in DMSO. Cell culture media, FCS, and antibiotics were obtained from Lonza (Basel, Switzerland) and Gibco (ThermoFisher Scientific, Waltham, MA). Other reagents were of analytic or molecular biological grade and were purchased from Sigma-Aldrich or Roche (Basel, Switzerland).

Cutaneous Telangiectasia Biopsy of Patients With HHT

Patients from the HHT Unit of Bellvitge University Hospital with mutations in *ACVRL1* and who presented cutaneous telangiectasias were selected for the study. Genetic tests were performed by Health in Code (A Coruña, Spain) using next-generation sequencing. Six patients were selected consecutively, all of whom gave their signed informed consent. Severity of nosebleeds was measured according to the epistaxis severity score.¹⁹ Abnormal findings from CT or contrast transthoracic echocardiography with agitated saline solution were also recorded. Contrast transthoracic echocardiography was scored according to the 4-category grading system proposed by Barzilai et al.²⁰ A punch biopsy (3 mm) from a cutaneous telangiectasia on a finger was obtained under the usual conditions of sterility and hygiene. Samples were processed directly into test tubes with formaldehyde in encrypted form according to a code assigned to each patient. The study was approved by the Clinical Research Ethics Committee of Bellvitge University Hospital.

Immunohistochemistry Studies

Biopsies were fixed in buffered formalin, dehydrated, and embedded in paraffin. Tissue sections (3–4 μ m) were stained with hematoxylin–eosin for morphological analysis. Sections of formalin-fixed, paraffin-embedded biopsies were analyzed to determine the amount of expression of various proteins. Samples were deparaffinized in xylene and rehydrated in downgraded alcohols and distilled water. CD34 was stained after antigen retrieval performed under high-pressure conditions for 2 minutes in citrate buffer, pH 6, and incubated with 3% H₂O₂ for 10 minutes. Samples were then blocked with 1:20 goat serum for 1 hour followed by incubation at 4°C overnight with monoclonal mouse antibody antihuman CD34 (Dako, Carpinteria, CA). Sections were incubated with the specific secondary anti-mouse antibody EnVision (Dako), followed by the DAB developing system (Dako). pAKT, pNDRG1, pS6, and Ki-67 were stained after antigen retrieval performed under high-pressure conditions for 4 minutes in citrate buffer, pH 6.5, and incubated with 3% H₂O₂ for 10 minutes. Samples were then blocked with 0.3% BSA in PBS for 1 hour followed by incubation at 4°C overnight with polyclonal rabbit antibody antiphospho-NDRG1 (Thr 346, Cat. 5482; Cell Signaling Technology, Inc, Beverly, MA), polyclonal rabbit antiphospho-AKT antibody (Ser 473, Cat. 9271; Cell Signaling Technology, Inc), polyclonal rabbit antibody antiphospho-S6 (Ser 240/244, Cat. 4838; Cell Signaling Technology, Inc), or monoclonal rabbit antibody anti-Ki-67 (SP6, Cat. MA5-15420; ThermoFisher Scientific). Sections

were incubated with the specific secondary anti-rabbit antibody EnVision (Dako), followed by the DAB developing system (Dako). Samples were counterstained with hematoxylin and visualized under light microscopy. For all samples, negative controls were performed, in which the section followed exactly the same protocol but in the absence of primary antibody.

Animals

Control and heterozygous *ALK1* mice (strain C57BL/6)²¹ were housed and maintained in laminar flow cabinets under specific pathogen-free conditions. All the animal studies were approved by the local committee for animal care (DAAM 5766; Institut d'Investigació Biomèdica de Bellvitge). Where indicated, *ALK1* heterozygous animals were crossed with the *p110α* heterozygous animal.²² Class I PI3K signaling was inhibited in half of the pups by subcutaneous injection at 6:00 pm in P6 and 10:00 am in P7 with 20 μL of 15 mmol/L LY294002 (Calbiochem, Millipore, Billerica, MA) dissolved in DMSO. Retinas were harvested at 2:00 pm on P7. Control mice were injected with DMSO only.

Retina Immunofluorescence

Eyes were fixed in 4% paraformaldehyde for 2 hours at 4°C. Retinas were permeabilized in PBS containing 1% BSA and 0.3% Triton X-100 overnight at 4°C, followed by incubation when indicated with polyclonal rabbit antiendothelial nuclei marker Erg-1/2/3 antibody (Cat. SC-353; Santa Cruz, CA) or polyclonal rabbit antidesmin antibody (Cat. Ab15200; Abcam, Cambridge, United Kingdom) in permeabilization buffer overnight at 4°C. The following day, the eyes were washed 3× with PBS containing 0.1% tween, once in Pblec buffer (1% Triton X-100, 1 mmol/L CaCl₂, 1 mmol/L MgCl₂, and 1 mmol/L MnCl₂ in PBS, pH 6.8) for 30 minutes and then incubated for 2 hours at room temperature (RT) or overnight at 4°C in Pblec buffer containing Alexa-488 or Alexa-568 conjugated secondary antibodies (1:200) and isolectin GS-IB₄ (1:300; Molecular Probes; ThermoFisher Scientific). They were washed 3 more times with PBS containing 0.1% tween and flat mounted on microscope glass slides with Mowiol. We used a Leica SP5 for fixed confocal laser scanning microscopy. Images were analyzed with Image J-Software. To address specific endothelial cell proliferation, we injected 60 μL of 2 mmol/L of the proliferation marker EdU (Click-iT EdU Imaging Kit; Invitrogen, Life Technologies, MA) for 2 hours into P7 mice. After euthanization, we determined EdU-positive ECs after colabeling with the endothelial nuclei marker Erg-1/2/3 and IB4 (isolectin B4), following the manufacturer's instructions.

Cell Culture

Human umbilical vein endothelial cells (HUVECs; passages 1–7) were obtained from Lonza and routinely cultured in gelatin coated (1%) in EBM (Lonza) supplemented with 20% FCS, 50 U/mL penicillin, 50 μg/mL streptomycin sulfate, 3 μg/mL human EGF, 30 μg/mL gentamicin, 15 ng/mL amphoterin, 9 mg/mL bovine brain extract, 25 mg/mL ascorbic acid, and 1 μg/mL hydrocortisone.

For short treatments, cells at 80% confluence were starved in M199 without FCS for 16 hours and then treated or not as indicated for various times with 10 ng/mL of BMP9 or 10 ng/mL of VEGF, depending on the experiment.

siRNA Transfection

For siRNA experiments, control (siGENOME nontargeting siRNA pool, Cat. D-001206-13-05; Dharmacon, GE Healthcare Life Sciences, Buckinghamshire, United Kingdom) or human PTEN (phosphatase and tensin homolog) siRNAs (Cat. D-003023-05-0005; Dharmacon) was diluted in Opti-MEM I at a final concentration of 80 nmol/L. Lipofectamine RNAiMAX (Cat. 13778; Invitrogen) was also diluted in Opti-MEM I in a different tube and added to the siRNA mix. After incubating for 20 minutes at RT, the transfection reagent mix was added to HUVECs in suspension (resuspended in Opti-MEM I medium containing 10% FBS) and seeded in 6-well plates.

Cells were incubated with the reaction mix for 8 hours. At the end of the incubation, the medium was changed to complete EBM for additional 48 hours. Cells were starved in M199 without FCS for 16 hours and then pretreated or not with 10 ng/mL of BMP9 for 4 hours and finally treated or not with 10 ng/mL of VEGF for an additional 30 minutes. For cell growth experiments, immediately after transfection, 1×10⁴ cells were seeded in 24-well plastic plates (Corning, NY). The next day, the medium was changed to M199 with 0.5% FCS, and the cells were treated or not with 10 ng/mL of BMP9, 10 ng/mL of VEGF, or a combination of BMP9 and VEGF. Cells were counted in a Neubauer chamber after 48 hours. Measurements were made under all conditions in triplicate in at least 3 independent experiments.

Cell Growth Assay

1×10⁴ cells were seeded in 24-well plastic plates (Corning, NY). The next day, the medium was changed to M199 with 0.5% FCS, and the cells were treated or not with 10 ng/mL of BMP9, 10 ng/mL of VEGF, or a combination of BMP9 and VEGF and in the absence or the presence of 0.5 μM SF1670. Cells were counted in a Neubauer chamber on 2 occasions (48 and 72 hours). Measurements were made under all conditions in triplicate in at least 3 independent experiments.

BrdU Proliferation Assay

5×10⁴ HUVECs were cultured on glass coverslips in 12-well plastic plates. The next day, the medium was changed to M199 without FCS, and the cells were treated or not with 10 ng/mL of BMP9, 10 ng/mL of VEGF, or a combination of BMP9 and VEGF for 20 hours. In parallel, exponential HUVECs (with 20% FCS) were plated for 24 hours and treated or not with 10 ng/mL of BMP9 and in the absence or the presence of 0.5-μM LDN-212854. BrdU (10 mmol/L; Amersham Pharmacia Biotech, Cambridge, United Kingdom) was added to the culture medium during the last 4 hours. Cells were fixed in 4% paraformaldehyde for 10 minutes at RT, permeabilized for 10 minutes with TBS-T (25 mmol/L Tris-HCl pH 7.4, 150 mmol/L NaCl, 0.5% Triton X-100), blocked with TBS-T containing 2% BSA, and incubated with primary antibody against BrdU (1:100) at 4°C for 16 hours. The following day, cells were washed 3× with TBS-T and incubated with Alexa conjugated secondary antibodies for 2 hours at RT. DAPI was added in the final wash. Specimens were mounted in Mowiol. Cells were visualized in a Nikon-80I microscope.

Western Blotting

Cells were collected and washed twice in cold PBS and lysed for 15 minutes at 4°C in RIPA lysis buffer (10 mmol/L NaF, 40 mmol/L β-glycerophosphate, 200 μM sodium orthovanadate, 0.1 μg/μL benzamide, 100 μM phenylmethylsulfonyl fluoride, 1 μM pepstatin A, 1 μg/mL leupeptin, 4 μg/mL aprotinin, 1% NP-40, 0.1% SDS, 0.5% sodium deoxycholate in PBS 1X pH 7.4). Insoluble material was removed by centrifugation at 12000 g for 5 minutes at 4°C. Proteins were separated by SDS-PAGE and electrophoretically transferred to Immobilon-P membranes (Millipore) in 25 mmol/L Tris-HCl, 0.19 mol/L glycine, and 10% methanol. Membranes were blocked in Tris-buffered saline, which is also known as TBS (50 mmol/L Tris, pH 7.4, 150 mmol/L NaCl), containing 5% nonfat dry milk for 1 hour at RT. Blots were incubated with 1:1000 polyclonal rabbit antiphospho-Smad1/5 (Ser 463/465) antibody (Cat. 9516; Cell Signaling Technology, Inc), 1:1000 monoclonal rabbit anti-Smad1 antibody (Cat. Ab33902; Abcam), 1:1000 polyclonal rabbit anti-ID1 (inhibitor of differentiation 1) antibody (Cat. SC-488; Santa Cruz), 1:1000 polyclonal rabbit anti-pVEGFR2 (Tyr 1175) antibody (Cat. 2478; Cell Signaling Technology, Inc), 1:1000 polyclonal rabbit anti-VEGFR2 antibody (Cat. 2479; Cell Signaling Technology, Inc), 1:1000 rabbit polyclonal antiphospho-AKT (Ser 473) antibody (Cat. 9271; Cell Signaling Technology, Inc), 1:1000 rabbit polyclonal antiphospho-AKT (Thr 308) antibody (Cat. 4056; Cell Signaling Technology, Inc), 1:1000 rabbit polyclonal anti-AKT antibody (Cat. 9272; Cell Signaling Technology, Inc), 1:1000 polyclonal rabbit antiphospho-p38 antibody (Cat. V1211; Promega, Madison



WI), 1:1000 polyclonal rabbit anti-p38 antibody (Cat. SC-728; Santa Cruz), 1:1000 rabbit polyclonal anti-PTEN antibody (Cat. 9559; Cell Signaling Technology, Inc), 1:3000 monoclonal mouse antitubulin antibody (Cat. T6074; Sigma Chemical), or 1:3000 monoclonal mouse antivinculin antibody (Cat. V9131; Sigma Chemical), in TBS 1% nonfat dry milk. After washing in TBS, 0.1% Triton, blots were incubated with anti-rabbit Ig (Amersham Pharmacia Biotech) or anti-mouse Ig (Amersham Pharmacia Biotech) horseradish peroxidase linked antibodies in blocking solution for 1 hour and developed with an enhanced chemiluminescence system (Amersham Pharmacia Biotech). Volumetric analysis was performed using the Quantity One volume analysis tool (Bio-Rad, CA).

PTEN Activity

HUVECs were starved in M199 without FCS for 16 hours and then pretreated or not with 10 ng/mL of BMP9 for 4 hours and finally treated or not with 10 ng/mL of VEGF for an additional 30 minutes. Cells were collected, washed twice in cold PBS, and lysed for 15 minutes at 4°C in NP-40 lysis buffer (50 mmol/L Tris, 150 mmol/L NaCl, 10% glycerol, 0.1 µg/µL benzamide, 100 µM phenylmethylsulfonyl fluoride, 1 µM pepstatin A, 1 µg/mL leupeptin, 4 µg/mL aprotinin, 0.2% NP-40, pH 7.4). Insoluble material was removed by centrifugation at 12000 g for 5 minutes at 4°C. To immunoprecipitate PTEN, 750 µg of total protein was first precleared by incubation for 4 hours at 4°C on an orbital shaker with 15 µL of protein A-Sepharose beads (GE Healthcare) and 15 µL of protein G-Sepharose beads (GE Healthcare). Beads were then discarded after centrifugation, and lysates were incubated with 2 µL of the rabbit polyclonal anti-PTEN antibody (Cat. 9559; Cell Signaling Technology, Inc) overnight at 4°C on the orbital shaker, with the exception of the negative controls that were incubated without antibody. Then lysates were incubated for 4 hours at 4°C on the orbital shaker with 15 µL of protein A-Sepharose beads (GE Healthcare) and 15 µL of protein G-Sepharose beads (GE Healthcare), previously cleaned with NP-40 buffer. Immunoprecipitates were then collected by centrifugation, washed 3× with NP-40 buffer at 4°C and once with PTEN Reaction buffer (Echelon Biosciences, Salt Lake City, UT). After immunoprecipitation, PTEN phosphatase activity was immediately measured in the bead complex using a PTEN activity ELISA (Cat. K-4700; Echelon Biosciences). PTEN activity was estimated by the percentage conversion from the initial PI(3,4,5)P₃ to PI(4,5)P₂ per assay point.

Quantitative Real-Time Polymerase Chain Reaction

Total RNA from HUVECs was extracted using TRIzol Reagent (Ambion, ThermoFisher Scientific). cDNA was obtained from a reverse transcription reaction (High-Capacity cDNA Reverse Transcription Kit; Applied Biosystems, Life Technologies, CA). Real-time polymerase chain reaction of cDNA obtained was performed on a LightCycler instrument (Roche Molecular Biochemicals, Lewes, United Kingdom). After initial incubation at 95°C for 10 minutes, 40 cycles of amplification were performed with denaturation at 95°C for 10 seconds, followed by annealing for 20 seconds (at 64°C) and extension at 72°C for 13 seconds. The ΔC_t values were calculated after subtracting the mean C_t values of the *RPL32* gene from PTEN mean C_t values. Results are presented as values of $2^{-(\Delta\Delta C_t)}$ relative to basal values.

The human-specific primers used were *PTEN* (5'-GTTTACCGCCAGCATCAAAAT-3' and 5'-CCCCCACTTTAGTGCAC-3') and the housekeeping gene *RPL32* (5'-CAGGTTTCGTAGAAGATTCAA GGG-3' and 5'-CTTGGAGGAAACATTGTGAGCGATC-3').

Gene Expression Analysis

Preprocessed and normalized gene expression data from telangiectasial or normal human tissue was obtained from the Gene Expression Omnibus reference GSE53515.²³ The rank-based analysis was based on the Gene Set Expression Analysis²⁴ tool using standard parameters.

The ranking of expression differences between telangiectasial and normal HHT2 tissue was based on the computed T statistic of paired samples. Two of the analyzed gene sets corresponded to independently curated annotations of the PI3K-AKT-mTOR signaling pathway (Hallmark PI3K-AKT-MTOR signaling and [Pathway Interaction Database] PI3KCI-AKT, included in Gene Set Expression Analysis MSigDB), and a third one corresponded to genes significantly overexpressed (false discovery rate, <5%) by oncogenic *PI3KCA* mutations in a nontumorigenic epithelial cell model (GSE33403).

Statistical Analysis

Statistical significance of group differences was determined using 2-tailed Mann-Whitney *U* tests (**P*<0.05, ***P*<0.01, ****P*<0.001, *****P*<0.0001). In the case of multiple group analysis, we have used Kruskal-Wallis test to assay differences between groups. Correlation between cutaneous telangiectasia biopsy positivity for pNDRG1 and nosebleed severity measured by the Epistaxis Severity Score was analyzed using 2-tailed Pearson correlation (*P*<0.01). Analyses were done using GraphPad Prism (v5.0b).

Results

Heterozygous Loss of *ALK1* Results in Retinal Vascular Hyperplasia

To gain insight into the molecular mechanism accounting for vascular malformations on loss of *ALK1* function in patients with HHT, we investigated vessel growth in postnatal mouse retinas. *ALK1*^{-/-} mice die in midgestation,^{12,13} so we studied heterozygous *ALK1*^{+/-} retinas. Whole-mount IB4-stained *ALK1*^{+/-} retinas showed no differences in vascular radial expansion or the number of branch points compared with wild-type littermates' retinas at postnatal days 5 (P5), 7, and 9 (Figure 1; Figure I in the online-only Data Supplement). In contrast, a partial decrease in *ALK1* levels resulted in vessel hyperplasia, as indicated by increased vessel width (Figure 1). Vessel hyperplasia in *ALK1*^{+/-} retinas occurred in capillary areas located above veins at P5, P7, and P9, whereas the effect was only observed in capillary areas located above arteries at P9 (Figure 1). Together, these findings indicate that *ALK1* signaling limits vessel width in sprouting angiogenesis, but it is not necessary for EC migration and til/stalk election. Although *ALK1*^{+/-} retinas have a mild vascular phenotype, they partially recapitulate the phenotype of full inactivation of *ALK1* in endothelial cells,²⁵ demonstrating a dose-response effect of *ALK1* in endothelial cells.

Coverage by mural cells regulates vessel diameter. Hence, the increase in vessel width induced by *ALK1* inhibition could be a consequence of reduced coverage by mural cells.^{26,27} However, immunostaining with desmin—a marker for retinal pericytes—did not reveal any obvious difference between wild-type and *ALK1*^{+/-} retinas (Figure II in the online-only Data Supplement). Next, we examined whether an increase in endothelial cell number could account for the increase in vessel width on heterozygous loss of *ALK1*. To this end, wild-type and *ALK1*^{+/-} retinas were stained with Erg-1/2/3—an endothelial-specific nuclear marker. Surprisingly, no differences were observed in the frequency of endothelial cells located in the inner retinal zone or in the first migratory endothelial cell line (mainly tip cells)²⁸ (Figure 2A and 2B). Conversely, an accumulation of 25% more endothelial cells was observed in the subfront (mainly formed of stalk cells) of *ALK1*^{+/-} retinas compared

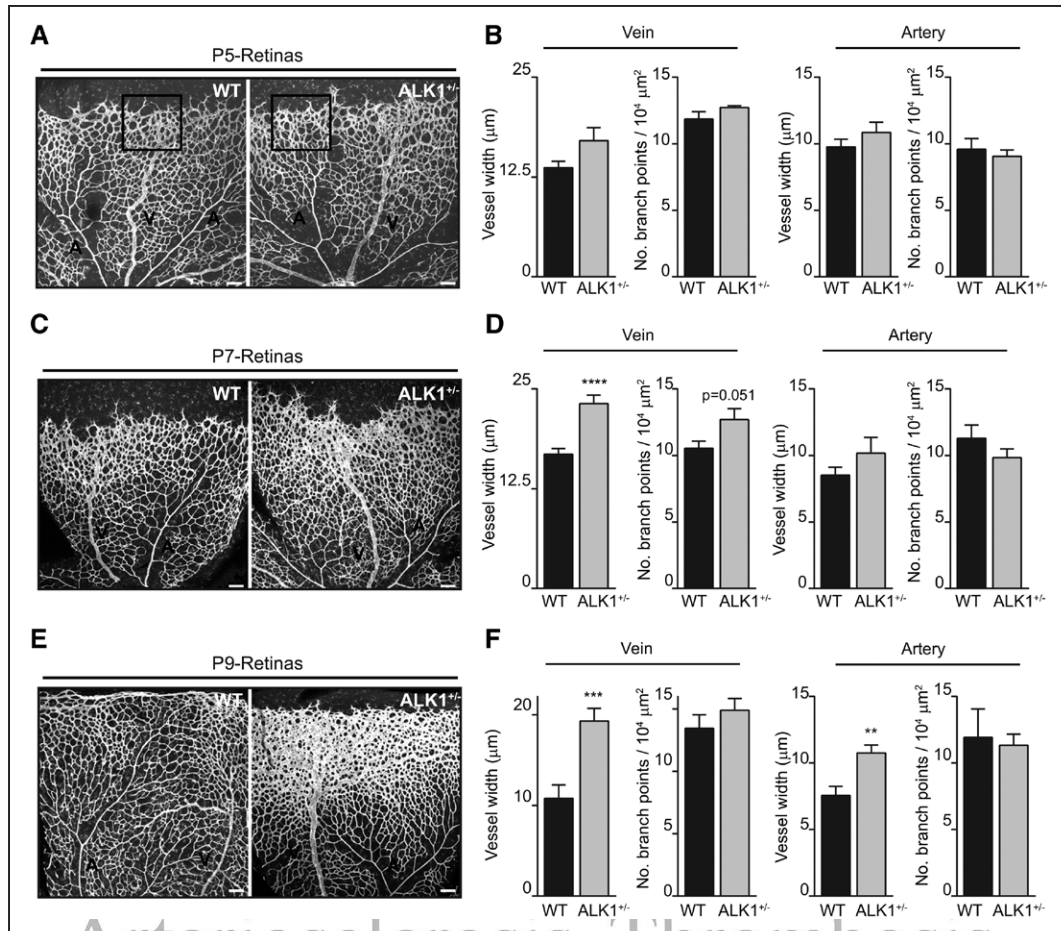


Figure 1. Heterozygous loss of *ALK1* results in retinal vascular hyperplasia. **A**, Whole-mount visualization of blood vessels by isolectin B4 staining of WT (wild type) or *ALK1*^{+/-} mice at P5. Red and green islets show venous and arterial selected regions where quantification analysis was done. **B**, Quantification of vessel width and number of branch points in veins and arteries of WT (n=8) and *ALK1*^{+/-} (n=7) retinas at P5. **C**, Whole-mount visualization of blood vessels by isolectin B4 staining of WT or *ALK1*^{+/-} mice at P7. **D**, Quantification of vessel width and number of branch points in veins and arteries of WT (n=28) and *ALK1*^{+/-} (n=27) retinas at P7. **E**, Whole-mount visualization of blood vessels by isolectin B4 staining of WT or *ALK1*^{+/-} mice at P9. **F**, Quantification of vessel width and number of branch points in veins and arteries of WT (n≥3) and *ALK1*^{+/-} (n=10) retinas at P9. Error bars indicate the standard error of the mean. A indicates artery and V, vein. Statistical significance of 2-tailed Mann–Whitney *U* tests: ***P*<0.01, ****P*<0.001, *****P*<0.0001.

with wild-type retinas. To establish whether this greater number was caused by an increase in endothelial cell proliferation, retinas were costained with Erg-1/2/3 and Edu (a proliferation marker; Figure 2A and 2C). Consistently, no differences were observed in the number of proliferative endothelial cells located in the internal vascular retinal area and in the first migratory endothelial line. Instead, a 41% higher frequency of proliferative endothelial cells was observed in the subfront of *ALK1*^{+/-} retinas, indicating that *ALK1* signaling restricts endothelial cell proliferation in vivo at the sprouting front.

BMP9 Blocks VEGF-Induced Proliferation in HUVECs

To understand the mechanisms by which *ALK1* prevents cell cycle progression in endothelial cells, we used cultured HUVECs and studied the crosstalk between BMP9 and angiogenic signals, such as VEGF. First, we stimulated HUVECs with VEGF, BMP9, or a combination of both, for 48 or 72 hours, followed by assessment of the total number of cells. Although BMP9 alone did not change the growth of HUVECs,

VEGF promoted a 37% increase in cell number after 48 hours and a 326% after 72 hours (Figure 2D). However, VEGF failed to stimulate cell number in the presence of BMP9. To confirm that BMP9 blocks cell proliferation without stimulating cell death, we measured BrdU incorporation in quiescent HUVECs in the presence of BMP9 and VEGF. As expected, stimulation with VEGF led to a greater degree of BrdU incorporation in HUVECs (Figure 2E) compared with nonstimulated conditions. We also found that BrdU incorporation was reduced by BMP9 stimulation in basal and VEGF-stimulated cells. BMP9 addition also reduced cell proliferation in complete medium (20% FCS). In agreement with the negative BMP9-*ALK1* role, addition of LDN-212854—an *ALK1* inhibitor—increased BrdU incorporation in HUVEC alone and reverted the inhibition caused by BMP9 (Figure 2E).

BMP9 Dampens VEGF-Induced Activation of AKT and ERKs

Next, we analyzed the effect of 15-minute or 4-hour BMP9 pretreatment in VEGF-mediated activation of PI3K-AKT,

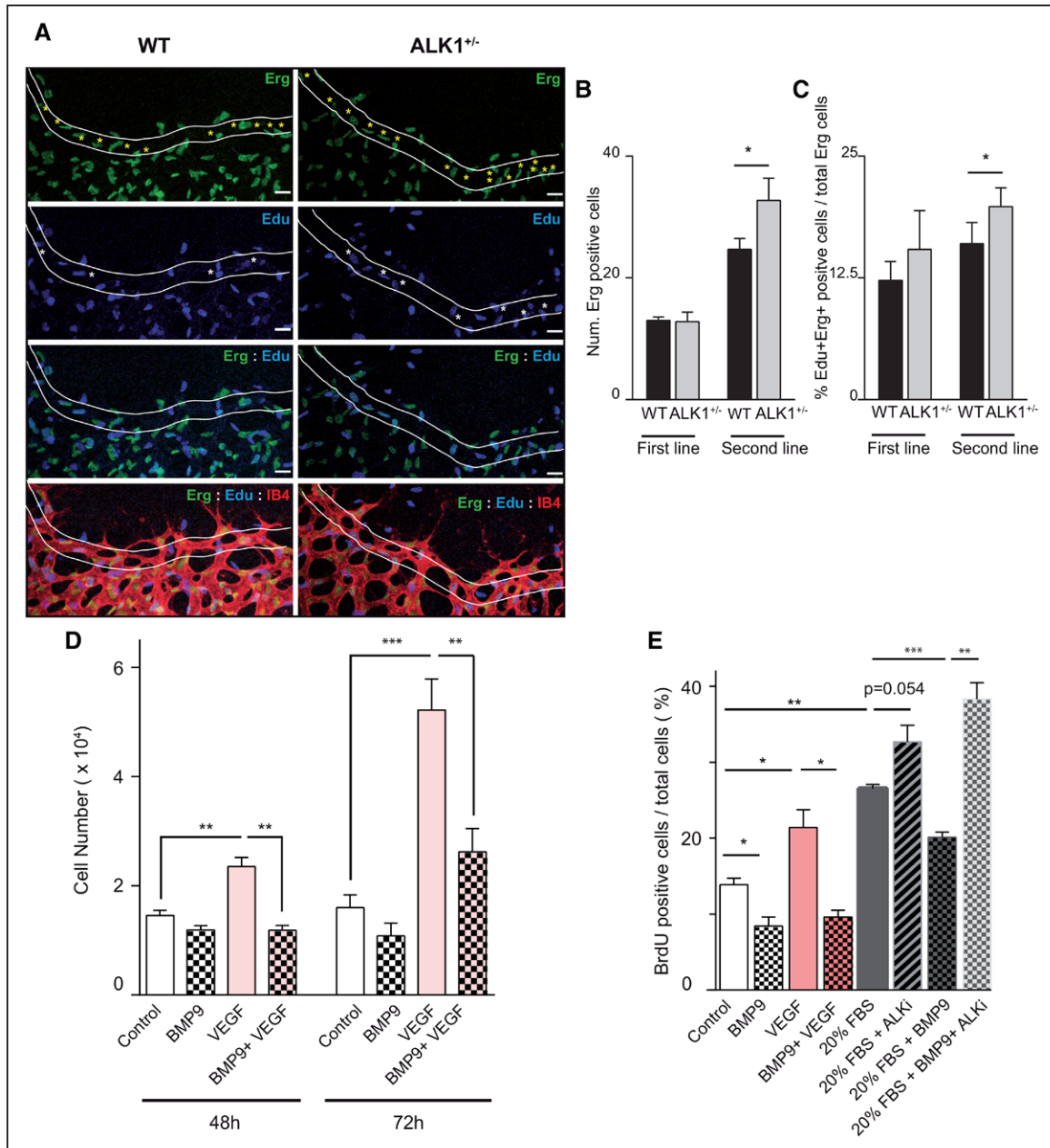


Figure 2. ALK1 (activin receptor-like kinase 1) negatively regulates endothelial cell proliferation in vitro and in vivo. **A**, Representative images of WT (wild type) and *ALK1*^{-/-} retinas immunostained with Erg-1/2/3 (green), Edu (blue), and isolectin B4 (red). Lines indicate the separation (20 μ m) between the 2 areas of quantification: first line (tip and first neighboring cells) and second line (second and third neighboring cells); scale bars=20 μ m). Yellow and white asterisks indicate Erg- and Edu-positive cells, respectively, located on the second line. **B**, Bars show quantification of endothelial nuclei per unit area assessed by Erg positivity in WT (n=11) and *ALK1*^{-/-} (n=6) retinas at P7. **C**, Quantification of percentage of proliferative endothelial cells (double Edu+/Erg+ with respect to total Erg+) in WT (n=11) and *ALK1*^{-/-} (n=6) retinas at P7. **D**, Human umbilical vein endothelial cells (HUVECs) were incubated for 48 or 72 h in medium 199 with 0.5% serum, in the presence or absence of 10 ng/mL VEGF (vascular endothelial growth factor), 10 ng/mL BMP (bone morphogenetic protein) 9 or 10 ng/mL VEGF, and 10 ng/mL BMP9, after which the cell number was counted. Each data point represents the mean of at least 3 independent experiments. **E**, Bars show quantification of proliferation of quiescent HUVECs plated for 24 h in the absence or presence of 10 ng/mL VEGF, 10 ng/mL BMP9 or 10 ng/mL VEGF, and 10 ng/mL BMP9, or exponential HUVECs (with 20% FCS) plated for 24 h in the absence or presence of 0.5 μ M LDN-212854 and in the absence or presence of 10 ng/mL BMP9. Cells were pulsed with BrdU for 4 h and subjected to immunostaining analysis. Results shown are the means of 4 independent experiments. Error bars indicate the standard errors of the mean. Statistical significance of 2-tailed Mann-Whitney *U* tests: **P*<0.05, ***P*<0.01, ****P*<0.001.

ERK (extracellular signal-regulated kinase) 1/2, and p38. We used phosphoSMAD1/5 and total abundance of ID1 as read-out of BMP9/ALK1 signaling (Figure 3; Figures III and IV in the [online-only Data Supplement](#)). Stimulation with VEGF for 10 and 30 minutes triggered the phosphorylation of AKT

and ERK1/2. VEGF and BMP9 both stimulated p38 MAPK phosphorylation, with a synergistic effect on incubation when both were used (Figure 3; Figure IV in the [online-only Data Supplement](#)). Pretreatment with BMP9 for 15 minutes before VEGF incubation had no effect on AKT and ERK1/2

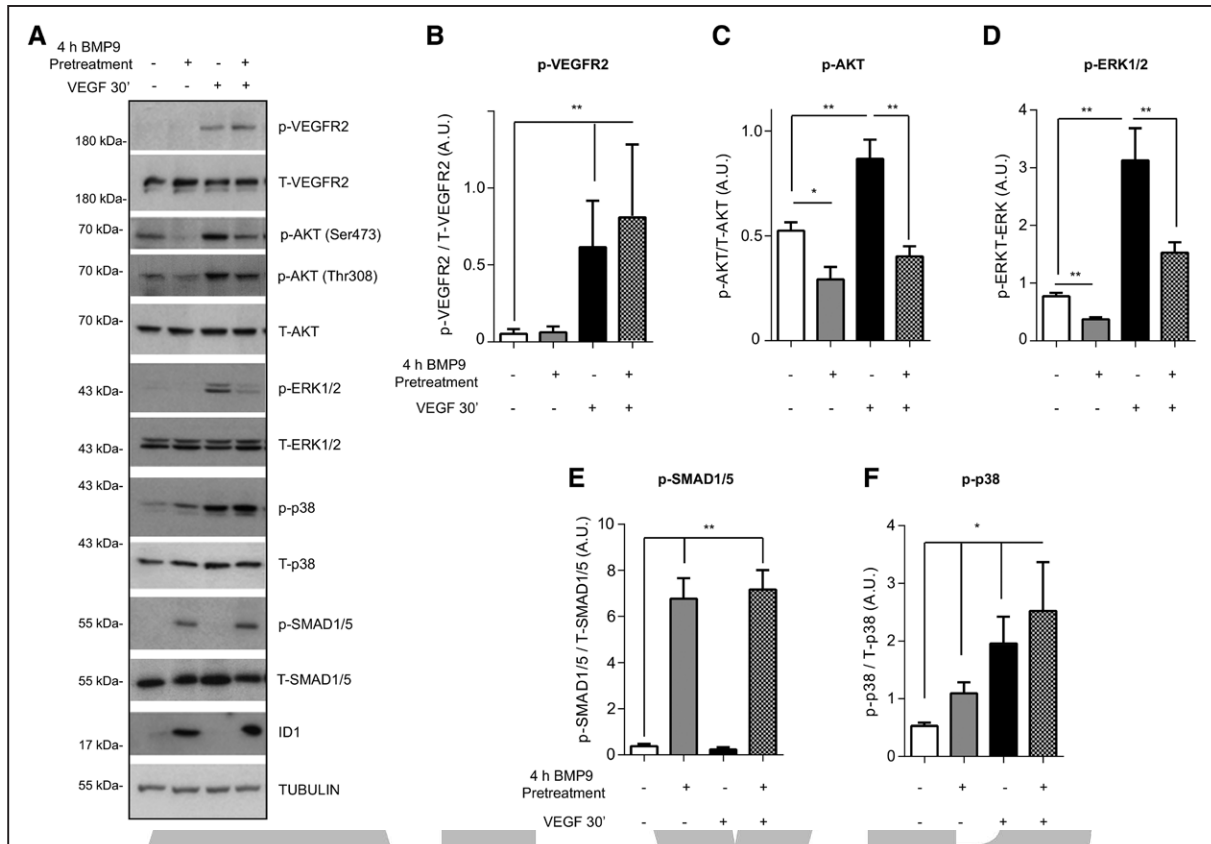


Figure 3. BMP (bone morphogenetic protein) 9 inhibits VEGF (vascular endothelial growth factor)-mediated activation of AKT and ERK (extracellular signal-regulated kinase). **A**, Growth factor-depleted human umbilical vein endothelial cells were pretreated with vehicle or 10 ng/mL BMP9 for 4 h, stimulated with VEGF for 30 min, and immunoblotted using the indicated antibodies. A representative blot of 5 independent experiments is shown. **B**, Bars show quantification of the relative immunoreactivity of phospho-VEGFR2 normalized with respect to total VEGFR2. The mean of 5 independent experiments is shown. **C**, Bars show quantification of the relative immunoreactivity of phospho-AKT (Ser473) normalized with respect to total AKT assessed as the mean of 5 independent experiments. **D**, Bars show quantification of the relative immunoreactivity of phospho-ERK1/2 normalized with respect to total ERK1/2. The mean of 5 independent experiments is shown. **E**, Bars show quantification of the relative immunoreactivity of phospho-SMAD1/5 normalized with respect to total SMAD1/5. The mean of 5 independent experiments is shown. **F**, Bars show quantification of the relative immunoreactivity of phospho-p38MAPK normalized with respect to total p38 MAPK. The mean of 5 independent experiments is shown. Error bars indicate the standard errors of the mean. Statistical significance of 2-tailed Mann-Whitney *U* tests: **P*<0.05, ***P*<0.01.

activation (Figure IVA in the [online-only Data Supplement](#)). Instead, a 4-hour preincubation with BMP9 blocked basal and VEGF-mediated phosphorylation of AKT (in threonine 308 and serine 473) and ERK1/2, without affecting the total amount of AKT or ERK1/2 protein or phosphorylation of VEGFR2 (Figure 3). This effect was dose-dependent, with a maximum effect achieved at a dose of 0.5 ng/mL of BMP9 in the absence of VEGF and of 5 ng/mL in the presence of VEGF (Figure IVC through IVE in the [online-only Data Supplement](#)). Moreover, a minimum of 2 hours time of preincubation with BMP9 was necessary to overrule the VEGF-mediated activation of AKT and ERKs (Figure IV in the [online-only Data Supplement](#)). We then sought to determine whether preincubation with VEGF also impaired the BMP9 canonical signaling pathway. However, BMP9-induced phosphoSMAD1/5 and ID1 expression were not altered if the cells had been preincubated with VEGF for 1 hour before adding BMP9 (Figure V in the [online-only Data Supplement](#)). Taken together, our data findings indicate that BMP9/ALK1 fine-tunes VEGF signaling, but this proangiogenic cue has no effect in modulating BMP9 signaling. Our results identify

BMP9 as a negative modulator of proangiogenic signals in endothelial cells.

BMP9 Inhibits PI3K Signaling by Increasing PTEN Activity

The PI3K/PTEN axis,^{28,29} but not ERK1/2 signaling,³⁰ has been shown to regulate endothelial cell proliferation in mouse retina angiogenesis. Furthermore, loss of PTEN in endothelial cells results in vascular hyperplasia similar to that observed in *ALK1*^{-/-} retinas.²⁸ Therefore, we hypothesized that BMP9 fine-tunes PI3K signaling by regulating PTEN. To confirm this, we first measured PTEN phosphatase activity. PTEN was immunoprecipitated from endothelial cells treated or not with BMP9 for 4 hours and additional 30 minutes with VEGF, and PTEN activity was quantified by its capacity to dephosphorylate PI(3,4,5)P₃ to PI(4,5)P₂. BMP9 treatment promoted a 48% increase in PTEN phosphatase activity, and this effect was independent of the presence or not of VEGF (Figure 4A). Next, we measured protein abundance after BMP9 treatment. Our results showed that PTEN amounts were maintained by a 4-hour treatment with BMP9 but increased substantially (86%)

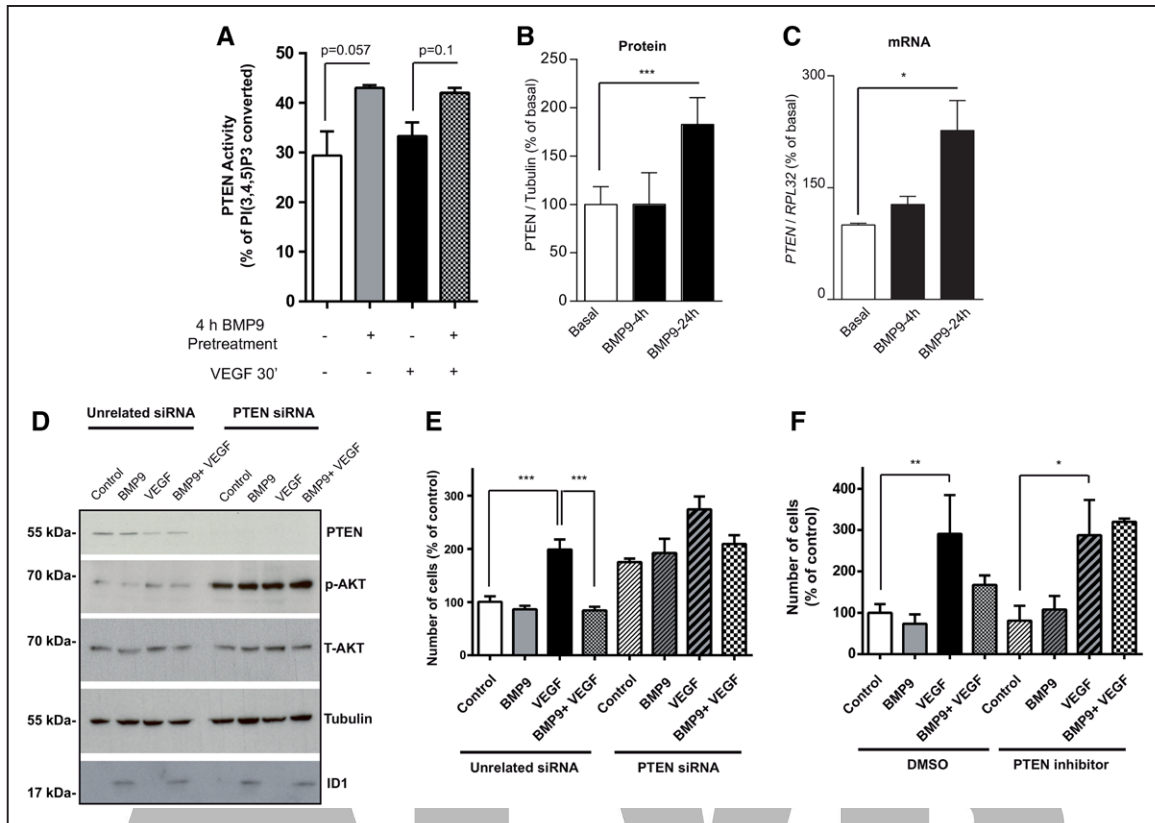


Figure 4. BMP (bone morphogenetic protein) 9 effects are mediated by PTEN (phosphatase and tensin homolog). **A**, Growth factor-depleted human umbilical vein endothelial cells (HUVECs) were pretreated with vehicle or 10 ng/mL BMP9 for 4 h and stimulated or not with VEGF (vascular endothelial growth factor) for 30 min. Cells were lysed, PTEN immunoprecipitated, and PTEN phosphatase activity measured by evaluating the conversion of PI(3,4,5)₃ to PI(4,5)₂, by ELISA. Results are expressed as the percentage conversion of initial PI(3,4,5)₃ to PI(4,5)₂. The mean of 4 independent experiments is shown. **B**, Growth factor-depleted HUVECs were treated with vehicle or 10 ng/mL BMP9 for 4 or 24 h and immunoblotted using appropriated antibodies. Bars show quantification of PTEN protein amount in basal situation (n=10) or induced by BMP9 for 4 (n=5) or 24 h (n=10) and normalized with respect to tubulin. **C**, Bars show quantification of *PTEN* mRNA induced by BMP9 stimulation for 4 or 24 h and normalized with respect to *RPL32* gene. The mean of 4 independent experiments is shown. **D**, HUVECs were transiently transfected with an unrelated control siRNA (unrelated siRNA) or PTEN siRNA, as described. After 48 h, cells were depleted of growth factors for 16 h. Cells were pretreated or not with 10 ng/mL BMP9 for 4 h, and then stimulated for 30 min in the absence or presence of 10 ng/mL VEGF. Cells were lysed and immunoblotted using the indicated antibodies. A representative blot of 5 independent experiments is shown. **E**, After transfection with siRNAs, 1×10^4 cells were seeded in 24-well plastic plates in normal medium. The next day, the medium was changed to M199 with 0.5% FCS, and the cells were treated or not with 10 ng/mL of BMP9, 10 ng/mL of VEGF, or a combination of BMP9 and VEGF. After 48 h, the cell number was assessed. Each data point represents the mean of at least 8 independent experiments. **F**, HUVECs were incubated in medium 199 with 0.5% serum, in the presence or absence of 10 ng/mL VEGF, 10 ng/mL BMP9, 10 ng/mL VEGF, and 10 ng/mL BMP9, and in the absence or presence of 0.5 μ M SF1670 PTEN inhibitor. After 72 h, the cell number was counted. Each data point represents the mean of at least 4 independent experiments. Error bars indicate the standard errors of the mean. Statistical significance of 2-tailed Mann-Whitney *U* tests: **P*<0.05, ***P*<0.01, ****P*<0.001.

when cells were treated with BMP9 for 24 hours (Figure 4B; Figure VIA in the [online-only Data Supplement](#)). This effect was correlated with an increase in *PTEN* mRNA abundance induced by BMP9 (44% after 4 hours and 184% after 24 hours of BMP9 treatment; Figure 4C). To confirm that PTEN was important for the inhibitory effect of BMP9 on AKT, we blocked its expression in HUVECs by siRNA transfection. The siRNAs acting against PTEN reduced PTEN protein amount and led to hyperactivation of the PI3K/AKT pathway (Figure 4D; Figure VIB in the [online-only Data Supplement](#)). More importantly, PTEN depletion abolished the inhibitory effects of BMP9 on AKT phosphorylation in basal and VEGF-stimulated cells, confirming that PTEN plays a critical role in BMP9-induced repression of PI3K/AKT. Next, we evaluated the effect of PTEN depletion on cell cycle progression in endothelial cells by assessment of the total number of cells.

Although VEGF failed to stimulate cell number in the presence of BMP9 in nonsilencing control cells, in the absence of PTEN, BMP9 was not able to block VEGF-induced cell proliferation (Figure 4E). We confirmed this result by incubating HUVEC with a PTEN inhibitor, SF1670. This compound also blocked the inhibitory effect of BMP9 on VEGF-induced endothelial cell number (Figure 4F), further supporting that PTEN activity is necessary to mediate BMP9 effects.

Activation of the PI3K Pathway in Cutaneous Telangiectasia Biopsies of Patients With HHT2

Having identified the mechanism of action of negative regulation by BMP9 signaling on proangiogenic signals, next we aimed to study the status of the PI3K pathway in samples from HHT2-affected individuals. To this end, we first examined publicly available gene expression data from nasal tissue

of HHT2-affected and control individuals (21 and 19, respectively²³). Using a rank-based algorithm,²⁴ a significant bias toward overexpression of genes linked to PI3K/AKT signaling (measured with 3 gene sets) was observed in telangiectasial tissue relative to normal tissue of patients with HHT2 (P values <0.01 ; Figure 5A; Table I in the [online-only Data Supplement](#)). Significant overexpression of these sets was also observed when comparing data of telangiectasial HHT2 tissue against normal tissue obtained from healthy individuals but not when comparing normal HHT2 against normal tissue of healthy individuals.²³

Next, we analyzed cutaneous telangiectasia biopsies from 6 patients with HHT2 with mutations in the *ACVRL1* gene (Table) and from 3 controls. We performed immunohistochemistry for CD34 (an endothelial cell marker), pAKT (S473), pNDRG1 (Thr 346), and pS6 (S240/244; markers of PI3K activation).^{31,32} As shown in Figure 5B and 5C, we found a 53% increase of vessels that were positive for pAKT. Moreover, a low frequency of control vessels were positive for pNDRG1 (3%; Figure 5B and 5D). In contrast, in the telangiectasia cohort, we found a 5-fold greater frequency of vessels that were positive for pNDRG1. Similarly, although endothelial cells from control biopsies were negative for pS6 staining, we found a 7-fold greater frequency of endothelial cells that were positive for pS6 (Figure 5B and 5E). Interestingly, we found a statistically significant positive correlation between grade of positivity for pNDRG1 and nosebleed severity measured by the epistaxis severity score (Table; Figure VII in the [online-only Data Supplement](#)).

Patients with HHT present enlarged abnormal vessels with high number of endothelial cells (Figure 5B). We asked whether mutations in *ALK1* also increased endothelial cell proliferation in vessels from patients with HHT2, as observed in our mouse model. We performed immunohistochemistry for Ki-67—a proliferation marker—in our HHT2 patient group and compared it with controls. Results indicated that the mean proliferation index was 3.3 \times significantly higher in endothelial cells from telangiectasias of patients with HHT2 than in control vessels (2.3 versus 0.7, respectively; Figure 5B and 5F).

Inhibition of PI3K Prevents Vascular Hyperplasia Induced by Loss of *ALK1* Expression

Finally, we examined whether inhibition of PI3K signaling can revert the vascular hyperplasia phenotype induced by heterozygous loss of *ALK1* in vivo. To this end, we crossed *ALK1*^{+/-} heterozygous animals with a constitutive mouse line in which endogenous p110 α /PI3K isoform is converted into kinase-dead protein (hereafter *p110 α ^{KD/WT}*).²² Although homozygous *p110 α ^{KD/KD}* mice die during embryonic development as a consequence of vascular failure, heterozygous inactivation of p110 α results in mild reduction of radial expansion³³—an effect that was maintained in double-heterozygous mutant retinas (*ALK1*^{+/-}; *p110 α ^{KD/WT}*; Figure VIII in the [online-only Data Supplement](#)). Instead, reduced p110 α activity rescued the hyperplasia induced by heterozygous loss of *ALK1* (Figure 6A and 6B). We validated these results by pharmacological inhibition of PI3K signaling with LY294002—a pan-PI3K inhibitor. Pups were treated with LY294002 at P6 and P7 (Figure 6C), and their retinal vasculature was examined at P7. The hyperplasia induced by *ALK1* heterozygosity was also rescued by pharmacological inhibition of PI3K activity

(Figure 6D and 6E). Taken together, these results confirm that BMP9/*ALK1* regulates endothelial cell proliferation in vivo, at least partially, by inhibiting PI3K/AKT signaling.

Discussion

In the present study, we demonstrate that BMP9/*ALK1* promotes vascular quiescence by inhibiting PI3K/AKT and ERK MAPK activation and show that loss of *ALK1* causes overstimulation of these signaling hubs. In recent years, the role of the BMP9-BMPRII-*ALK1*-endoglin-SMAD1/5 axis in endothelial cells has begun to be clarified.^{34,35} Indeed, BMP9/*ALK1* inhibits cell proliferation and migration in cultured endothelial cells^{10,36,37} and in zebrafish.³⁸ In mice, the blockade of BMP9/*ALK1* signaling by anti-BMP9 neutralizing antibody or by injection of the extracellular domain of *ALK1* increases vascular density.³⁹ Also, in mice, depletion of *ALK1* specifically in endothelial cells results in AVMs as a result of increased endothelial cell proliferation.^{25,40–42} Our results in vitro and in vivo confirm this antiproliferative role of BMP9/*ALK1* in sprouting angiogenesis. Our work also reveals that during vessel growth, BMP9/*ALK1* signaling does not regulate cell proliferation in all angiogenic endothelial cells in vivo but, rather, specifically in those cells located at the sprouting. Activation of Notch at the sprouting front results in stalk cell cycle arrest²⁸ through a similar mechanism to that of BMP9/*ALK1* (see below). It is, therefore, reasonable to speculate that Notch and BMP9/*ALK1* cooperate to restrain stalk cell proliferation at this specific location. In keeping with this, previous results have shown that *ALK1*, through SMAD1/5^{43,44} or SMAD2/3 activation,⁴⁵ cooperates with the Dll4/Notch pathway to induce the stalk cell phenotype.

Our in vitro and in vivo findings place PI3K/AKT and ERK MAPK at the center of the BMP9/*ALK1* antiproliferative response (Figure IX in the [online-only Data Supplement](#)). Our results using HUVECs as a model have shown that BMP9/*ALK1* blocks the PI3K/AKT and ERK activation induced by VEGF. In contrast, we have found that pharmacological inhibition of PI3K is sufficient to abolish *ALK1*-induced vascular hyperplasia in vivo. This observation, together with the fact that inhibitors of MEK1-ERKs in vivo fail to block endothelial cell proliferation in wild-type retinal angiogenesis,³⁰ suggests that limiting PI3K signaling is the principal mechanism by which *ALK1* stimulates vascular quiescence in vivo. The PI3K/AKT pathway stimulates cell proliferation, migration, and survival in endothelial cells downstream of many angiogenic cues.^{28,46} We have identified BMP9/*ALK1* as a new upstream signal that regulates PI3K activity in sprouting angiogenesis. Although most of the angiogenic cues activate the PI3K signaling pathway to execute their biological actions, we have found that BMP9/*ALK1* represses this signaling cascade by stimulating the activity of PTEN—the principal phosphatase that counteracts this signaling pathway in endothelial cells.⁴⁶ PTEN is a lipid and protein phosphatase whose function is regulated at multiple levels, including mRNA and protein expression, subcellular localization, and direct regulation of its phosphatase activity by post-translational modifications, such as phosphorylation, ubiquitination, and protein interactions.^{47,48} We have identified that regulation of PTEN by BMP9/*ALK1* in endothelial cells is also multifactorial. First, the observation that BMP9/*ALK1* dampens AKT phosphorylation after a

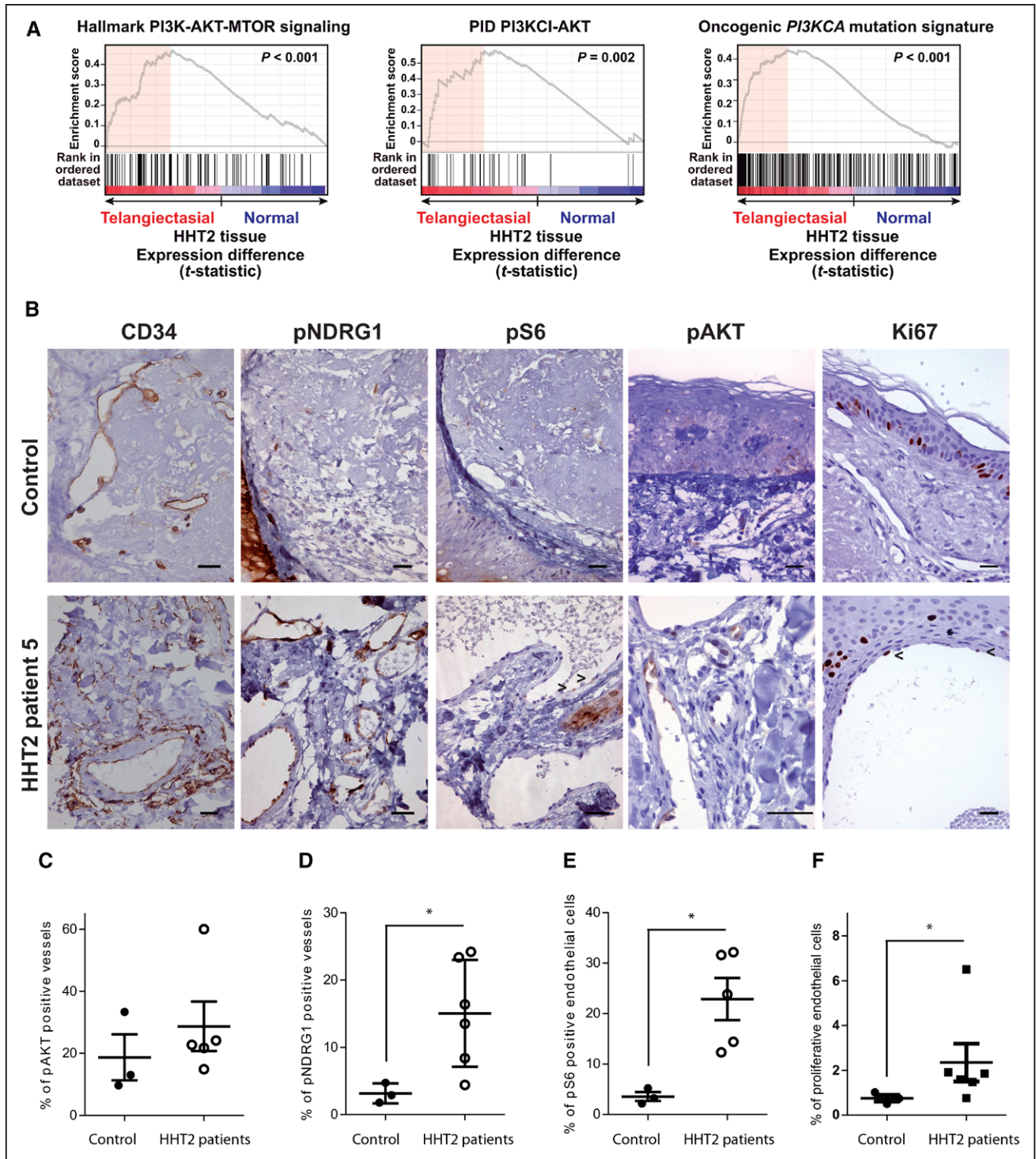


Figure 5. Increased activation of PI3K (phosphatidylinositol 3-kinase) signaling and endothelial cell proliferation in hereditary hemorrhagic telangiectasia 2 (HHT2) cutaneous telangiectasia biopsies. **A**, Gene set expression analysis (GSEA) output plots showing significant over-expression of gene sets corresponding to PI3K-AKT-mTOR canonical annotations (Hallmark PI3K-AKT-MTOR signaling and PID PI3KCI-AKT) or genes significantly overexpressed by oncogenic *PI3KCA* mutations. The detailed results of each set are provided in Table I in the [online-only Data Supplement](#). The GSEA enrichment scores and the nominal *P* values are shown. The red-shadow areas mark the leading peaks that contribute to the associations. **B**, CD34, pNDRG1, pS6, pAKT, and Ki-67 (brown nuclei, arrows) staining of a control and a HHT2 patient (scale bars=100 μ m). **C**, Quantification of the percentage of pAKT-positive vessels in controls (n=3) and patients with HHT2 (n=5). **D**, Quantification of the percentage of pNDRG1-positive vessels in controls (n=3) and patients with HHT2 (n=6). **E**, Quantification of the percentage of pS6-positive endothelial cells in controls (n=3) and patients with HHT2 (n=5). **F**, Quantification of the percentage of Ki-67-positive endothelial cells in controls (n=3) and patients with HHT2 (n=6). Error bars indicate the standard errors of the mean. Statistical significance of 2-tailed Mann-Whitney *U* tests: * $P < 0.05$.

Table. Hereditary Hemorrhagic Telangiectasia 2 Patient Characteristics

Patient No.*	Age, y	M/F	Contrast TTE	Abdominal Computed Tomography	CI, L/min per m ²	ESS†	pNDRG1 Vessels, %	ACVRL1 Mutations
1	62	F	1	Intrahepatic telangiectasias	3.74	2.83	8.4	Exon 3: c.244_246 del ACC p.T82del
				Hepatic AV shunt				
				Hepatic artery enlargement				
				FNH				
				Intrapancreatic AVM				
				Ileal AVM				
				Caecal AVM				
Uterine AVM								
2	49	M	1	No pathological findings	2.28	6.38	23.4	Exon 3: change 229T>C Cys77Arg
3	41	F	3	Intrahepatic telangiectasias	3.12	2.93	4.4	Exon 10: change 1436G>C Arg479Pro*
				Hepatic AV shunt				
				Hepatic artery enlargement				
				NRH				
				Uterine AVM				
4	70	F	0	Hepatomegaly	3.7	6.59	24.2	Exon 10: change 1436G>C Arg479Pro*
				Hepatic AV shunt				
				Hepatic artery enlargement				
				Intrapancreatic AVM				
				Left renal artery aneurysm				
5	49	M	0	Intrahepatic telangiectasias	2.9	4.57	13.5	Exon 10: change 1436G>C Arg479Pro
				Intrapancreatic AVM				
				Gastro-omental artery aneurysms				
6	51	M	1	Hepatomegaly	3.3	6.05	16.4	Exon 10: 1450C>T Arg484Trp
				Hepatic AP shunt				
				Hepatic artery enlargement				

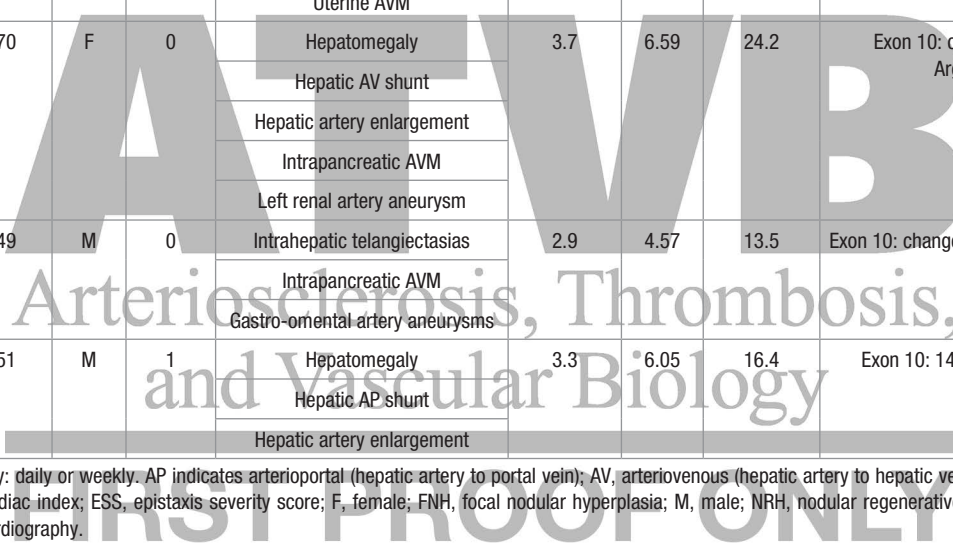
Epistaxis frequency: daily or weekly. AP indicates arterioportal (hepatic artery to portal vein); AV, arteriovenous (hepatic artery to hepatic vein); AVM, arteriovenous malformation; CI, cardiac index; ESS, epistaxis severity score; F, female; FNH, focal nodular hyperplasia; M, male; NRH, nodular regenerative hyperplasia; and TTE, transthoracic echocardiography.

*Patient 4 is the mother of patient 3.

2-hour incubation with BMP9 suggests a direct regulation of PTEN catalytic activity. Recently, Ola et al⁴⁷ have described that the phosphorylated Ser380/Thr382/Thr383-inactive form of PTEN was decreased in HUVECs and mLECs endothelial cells stimulated for 2 hours with BMP9.⁴² Second, we have clear evidence that stimulation of endothelial cells by BMP9/ALK1 increases mRNA and protein abundance of PTEN. This is not unique to BMP9/ALK1 because we have previously shown that Dll4/Notch also stimulates PTEN expression to block stalk cell proliferation.²⁸ Given the previously identified crosstalk between ALK1 and Notch, the increase in PTEN amount on BMP9 stimulation could be explained by an indirect response induced by Notch. However, we cannot rule out a direct effect of SMADs on *PTEN* promoter on BMP9 stimulation. PTEN expression is also tightly regulated by miR, including in endothelial cells. Indeed, VEGF restrains PTEN expression amount by increasing the expression of the miR-17 to 92 cluster in endothelial cells.⁴⁹ Therefore, it is also possible

that BMP9/ALK1 regulates PTEN abundance by inhibiting negative regulators of its expression. Taken together, we have identified a previously unknown interaction of BMP9/ALK1 and PTEN in endothelial cells, which seems critical to the pathogenesis of loss of ALK1 expression.

HHT is mainly caused by heterozygous mutations in *ENG*¹⁷ or *ALK1 (ACVRL1)*¹⁸ genes. These are loss-of-function mutations that lead to reduced BMP9/ALK1/endoglin/SMAD1/5 signaling and enhanced response to angiogenic cues and thereby to excessive abnormal angiogenesis.¹⁴ The telangiectasia arises from a postcapillary hyperplastic venule that fuses directly with an arteriole, resulting in an arteriovenous shunt in the small-sized vessels.¹⁵ The role of endothelial cell proliferation in the development of these enlarged abnormal vessels in HHT has not been studied in deep. Hashimoto et al⁵⁰ found higher Ki-67 index for endothelial cells of sporadic brain AVMs compared with endothelial cells from control cortical vessels. In the case of HHT, Du et al⁵¹ found increased



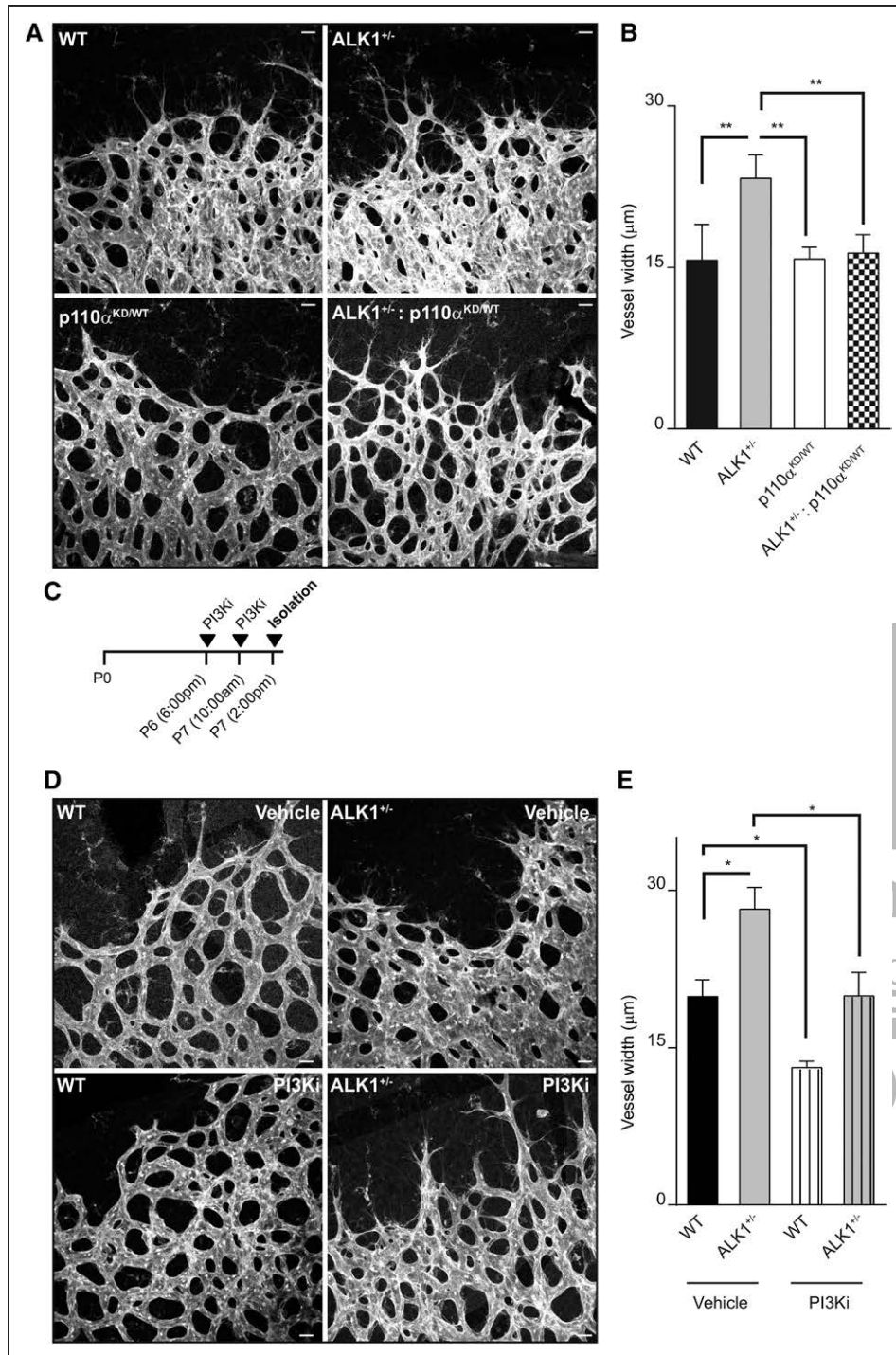


Figure 6. In vivo inhibition of PI3K (phosphatidylinositol 3-kinase) blocks vascular hyperplasia in *ALK1*^{+/-} retinas. **A**, Whole-mount visualization of blood vessels by isolectin B4 staining WT (wild type), *ALK1*^{+/-}, *p110α*^{KD/WT}, and double *ALK1*^{+/-}/*p110α*^{KD/WT} retinas at P7. **B**, Quantification of vessel width in veins of WT (n=4), *ALK1*^{+/-} (n=8), *p110α*^{KD/WT} (n=4), and double *ALK1*^{+/-}/*p110α*^{KD/WT} (n=6) retinas. **C**, Scheme of pharmacological approach to inhibit PI3K with LY294002. **D**, Isolectin B4 stained WT and *ALK1*^{+/-} treated with vehicle or LY294002 at P6 and P7. **E**, Quantification of the vessel width of retinas shown in **C**; n ≥4 per treatment and genotype. Error bars indicate the standard errors of the mean. Statistical significance of 2-tailed Mann-Whitney U tests: *P<0.05, **P<0.01.

endothelial cell proliferation in a resection of intracranial AVM in a 26-day-old boy with HHT. Our data obtained in patients, as well as the results obtained in mouse models, confirm that AVMs and increased endothelial cell proliferation are inter-related, suggesting that the AVM phenotype in patients with HHT arises, at least in part, from an aberrant endothelial cell proliferation. In line with this stimulation of VEGF signaling, a promitogenic factor for endothelial cells is required for the development of HHT. Indeed, although heterozygous *ALK1* mice do not develop AVM, intracranial injection of VEGF in *ALK1*^{+/-} mice leads to abnormal AVM-like structures,⁵² and

blocking VEGF attenuates these vascular lesions.⁵³ This is in agreement with the observation that PI3K/AKT is a key signaling hub downstream of VEGF in angiogenesis.⁴⁶ Our results show for first time an overstimulation of the PI3K pathway on vessels of patients with HHT2. We found a statistically significant relationship between PI3K-activated vessels in the finger telangiectasia biopsy and the severity of nosebleeds measured by the epistaxis severity score. This association suggests a more intense development of systemic telangiectasias (ie, cutaneous or in nasal mucosa) when PI3K signaling is active. It is of particular note that we and others have found that the

majority of venous malformations—the most common form of vascular malformation—are driven by constitutively activating PI3K signaling.^{29,54} Taken together, the results suggest that overactivation of PI3K signaling is a common characteristic in vascular malformations. By using a mouse model for HHT, our findings also show that the genetic or pharmacological inhibition of PI3K prevents ALK1-induced vascular hyperplasia in retinas. Our findings corroborate results in the study by Ola et al⁴² in which homozygous deletion of *ALK1* in endothelial cells results in arterial venous shunts also by upregulating PI3K signaling. These results suggest that PI3K inhibitors could be used as an alternative therapeutic approach to treat patients with HHT. Inhibition of the PI3K signaling in the vasculature could, therefore, prevent the development of telangiectasias and improve nose bleeds in patients with HHT. In keeping with this observation, a study has reported a clinical case of an HHT2 patient diagnosed with serous ovarian cancer who showed a drop in the frequency of epistaxis on treatment with a PI3K inhibitor (BKM120).⁵⁵ Therefore, we propose that the use of PI3K or AKT inhibitors should be considered as alternative pharmacological strategies for treating patients with HHT.

Acknowledgments

We thank K. Pietras (Lund University, Sweden) and S. Paul Oh (University of Florida) for the *ALK1* heterozygous animals. We are grateful to the subjects who participated in this study.

Sources of Funding

This study was supported by research grants from the Spanish Ministerio de Economía y Competitividad (SAF2013-46063-R and SAF2017-85869-R) and the Generalitat de Catalunya (2014SGR364) to F. Viñals. E. Alsina-Sanchís is a recipient of a predoctoral fellowship from the Ministerio de Economía y Competitividad. Work in M. Graupera's laboratory is supported by research grants SAF2014-59950-P and SAF2017-89116-R from the Spanish Ministerio de Economía y Competitividad (Spain), 2014-SGR-725 from the Catalan Government, the People Programme (Marie Curie Actions; grant agreement 317250) of the European Union Seventh Framework Programme FP7/2007 to 2013, the Marie Skłodowska-Curie grant (agreement 675392) of the European Union Horizon 2020 research and innovation programme, the project CB16/12/00445 (CIBERONCO), and from la Fundació Bancària "la Caixa".

Disclosures

The authors report an unrestricted grant from Roche to finance the ProCure Programme, which was paid to the Catalan Institute of Oncology (2015).

References

- Carmeliet P. Mechanisms of angiogenesis and arteriogenesis. *Nat Med*. 2000;6:389–395. doi: 10.1038/74651.
- Adams RH, Alitalo K. Molecular regulation of angiogenesis and lymphangiogenesis. *Nat Rev Mol Cell Biol*. 2007;8:464–478. doi: 10.1038/nrm2183.
- Carmeliet P, Jain RK. Molecular mechanisms and clinical applications of angiogenesis. *Nature*. 2011;473:298–307. doi: 10.1038/nature10144.
- Jain RK. Molecular regulation of vessel maturation. *Nat Med*. 2003;9:685–693. doi: 10.1038/nm0603-685.
- Gaengel K, Genové G, Armulik A, Betsholtz C. Endothelial-mural cell signaling in vascular development and angiogenesis. *Arterioscler Thromb Vasc Biol*. 2009;29:630–638. doi: 10.1161/ATVBAHA.107.161521.
- David L, Mallet C, Mazerbourg S, Feige JJ, Bailly S. Identification of BMP9 and BMP10 as functional activators of the orphan activin receptor-like kinase 1 (ALK1) in endothelial cells. *Blood*. 2007;109:1953–1961. doi: 10.1182/blood-2006-07-034124.
- Valdimarsdottir G, Goumans MJ, Rosendahl A, Brugman M, Itoh S, Lebrin F, Sideras P, ten Dijke P. Stimulation of Id1 expression by bone morphogenetic protein is sufficient and necessary for bone morphogenetic protein-induced activation of endothelial cells. *Circulation*. 2002;106:2263–2270.
- Somekawa S, Imagawa K, Hayashi H, Sakabe M, Ioka T, Sato GE, Inada K, Iwamoto T, Mori T, Uemura S, Nakagawa O, Saito Y. Tmem100, an ALK1 receptor signaling-dependent gene essential for arterial endothelium differentiation and vascular morphogenesis. *Proc Natl Acad Sci USA*. 2012;109:12064–12069. doi: 10.1073/pnas.1207210109.
- Nolan-Stevaux O, Zhong W, Culp S, Shaffer K, Hoover J, Wickramasinghe D, Ruefli-Brasse A. Endoglin requirement for BMP9 signaling in endothelial cells reveals new mechanism of action for selective anti-endoglin antibodies. *PLoS One*. 2012;7:e50920. doi: 10.1371/journal.pone.0050920.
- Scharpfenecker M, van Dinther M, Liu Z, van Bezooijen RL, Zhao Q, Pukac L, Löwik CW, ten Dijke P. BMP-9 signals via ALK1 and inhibits bFGF-induced endothelial cell proliferation and VEGF-stimulated angiogenesis. *J Cell Sci*. 2007;120(pt 6):964–972. doi: 10.1242/jcs.002949.
- Townson SA, Martinez-Hackert E, Greppi C, Lowden P, Sako D, Liu J, Ucran JA, Liharska K, Underwood KW, Seehra J, Kumar R, Grinberg AV. Specificity and structure of a high affinity activin receptor-like kinase 1 (ALK1) signaling complex. *J Biol Chem*. 2012;287:27313–27325. doi: 10.1074/jbc.M112.377960.
- Oh SP, Seki T, Goss KA, Imamura T, Yi Y, Donahoe PK, Li L, Miyazono K, ten Dijke P, Kim S, Li E. Activin receptor-like kinase 1 modulates transforming growth factor-beta 1 signaling in the regulation of angiogenesis. *Proc Natl Acad Sci USA*. 2000;97:2626–2631.
- Urness LD, Sorensen LK, Li DY. Arteriovenous malformations in mice lacking activin receptor-like kinase-1. *Nat Genet*. 2000;26:328–331. doi: 10.1038/81634.
- Choi EJ, Kim YH, Choe SW, Tak YG, Garrido-Martin EM, Chang M, Lee YJ, Oh SP. Enhanced responses to angiogenic cues underlie the pathogenesis of hereditary hemorrhagic telangiectasia 2. *PLoS One*. 2013;8:e63138. doi: 10.1371/journal.pone.0063138.
- Guttmacher AE, Marchuk DA, White RI Jr. Hereditary hemorrhagic telangiectasia. *N Engl J Med*. 1995;333:918–924. doi: 10.1056/NEJM199510053331407.
- Govani FS, Shovlin CL. Hereditary haemorrhagic telangiectasia: a clinical and scientific review. *Eur J Hum Genet*. 2009;17:860–871. doi: 10.1038/ejhg.2009.35.
- McAllister KA, Grogg KM, Johnson DW, Gallione CJ, Baldwin MA, Jackson CE, Helmbold EA, Markel DS, McKinnon WC, Murrell J. Endoglin, a TGF-beta binding protein of endothelial cells, is the gene for hereditary haemorrhagic telangiectasia type 1. *Nat Genet*. 1994;8:345–351. doi: 10.1038/ng1294-345.
- Johnson DW, Berg JN, Baldwin MA, et al. Mutations in the activin receptor-like kinase 1 gene in hereditary haemorrhagic telangiectasia type 2. *Nat Genet*. 1996;13:189–195. doi: 10.1038/ng0696-189.
- Hoag JB, Terry P, Mitchell S, Reh D, Merlo CA. An epistaxis severity score for hereditary hemorrhagic telangiectasia. *Laryngoscope*. 2010;120:838–843. doi: 10.1002/lary.20818.
- Barzilai B, Waggoner AD, Spessert C, Picus D, Goodenberger D. Two-dimensional contrast echocardiography in the detection and follow-up of congenital pulmonary arteriovenous malformations. *Am J Cardiol*. 1991;68:1507–1510.
- Srinivasan S, Hanes MA, Dickens T, Porteous ME, Oh SP, Hale LP, Marchuk DA. A mouse model for hereditary hemorrhagic telangiectasia (HHT) type 2. *Hum Mol Genet*. 2003;12:473–482.
- Foukas LC, Claret M, Pearce W, Okkenhaug K, Meek S, Peskett E, Sancho S, Smith AJ, Withers DJ, Vanhaesebroeck B. Critical role for the p110alpha phosphoinositide-3-OH kinase in growth and metabolic regulation. *Nature*. 2006;441:366–370. doi: 10.1038/nature04694.
- Tørring PM, Larsen MJ, Kjeldsen AD, Ousager LB, Tan Q, Brusgaard K. Long non-coding RNA expression profiles in hereditary haemorrhagic telangiectasia. *PLoS One*. 2014;9:e90272. doi: 10.1371/journal.pone.0090272.
- Subramanian A, Tamayo P, Mootha VK, Mukherjee S, Ebert BL, Gillette MA, Paulovich A, Pomeroy SL, Golub TR, Lander ES, Mesirov JP. Gene set enrichment analysis: a knowledge-based approach for interpreting genome-wide expression profiles. *Proc Natl Acad Sci USA*. 2005;102:15545–15550. doi: 10.1073/pnas.0506580102.
- Tual-Chalot S, Mahmoud M, Allinson KR, Redgrave RE, Zhai Z, Oh SP, Fruttiger M, Arthur HM. Endothelial depletion of Acvrl1 in mice leads to arteriovenous malformations associated with reduced endoglin expression. *PLoS One*. 2014;9:e98646. doi: 10.1371/journal.pone.0098646.

26. Park SO, Lee YJ, Seki T, Hong KH, Fliess N, Jiang Z, Park A, Wu X, Kaartinen V, Roman BL, Oh SP. ALK5- and TGFBR2-independent role of ALK1 in the pathogenesis of hereditary hemorrhagic telangiectasia type 2. *Blood*. 2008;111:633–642. doi: 10.1182/blood-2007-08-107359.
27. Mahmoud M, Allinson KR, Zhai Z, Oakenfull R, Ghandi P, Adams RH, Fruttiger M, Arthur HM. Pathogenesis of arteriovenous malformations in the absence of endoglin. *Circ Res*. 2010;106:1425–1433. doi: 10.1161/CIRCRESAHA.109.211037.
28. Serra H, Chivite I, Angulo-Urarte A, et al. PTEN mediates Notch-dependent stalk cell arrest in angiogenesis. *Nat Commun*. 2015;6:7935. doi: 10.1038/ncomms8935.
29. Castillo SD, Tzouanacou E, Zaw-Thin M, et al. Somatic activating mutations in Pik3ca cause sporadic venous malformations in mice and humans. *Sci Transl Med*. 2016;8:332ra43. doi: 10.1126/scitranslmed.aad9982.
30. Zhu T, Sennlaub F, Beauchamp MH, Fan L, Joyal JS, Checchin D, Nim S, Lachapelle P, Sirinyan M, Hou X, Bossolasco M, Rivard GE, Heveker N, Chemtob S. Proangiogenic effects of protease-activated receptor 2 are tumor necrosis factor-alpha and consecutively Tie2 dependent. *Arterioscler Thromb Vasc Biol*. 2006;26:744–750. doi: 10.1161/01.ATV.0000205591.88522.d4.
31. Firestone GL, Giampaolo JR, O'Keefe BA. Stimulus-dependent regulation of serum and glucocorticoid inducible protein kinase (SGK) transcription, subcellular localization and enzymatic activity. *Cell Physiol Biochem*. 2003;13:1–12. doi: 10.1159/000070244.
32. Murray JT, Campbell DG, Morrice N, Auld GC, Shpro N, Marquez R, Peggie M, Bain J, Bloomberg GB, Grahammer F, Lang F, Wulff P, Kuhl D, Cohen P. Exploitation of KESTREL to identify NDRG family members as physiological substrates for SGK1 and GSK3. *Biochem J*. 2004;384(pt 3):477–488. doi: 10.1042/BJ20041057.
33. Graupera M, Guillermet-Guibert J, Foukas LC, Phng LK, Cain RJ, Salpekar A, Pearce W, Meek S, Millan J, Cutillas PR, Smith AJ, Ridley AJ, Ruhrberg C, Gerhardt H, Vanhaesebroeck B. Angiogenesis selectively requires the p110alpha isoform of PI3K to control endothelial cell migration. *Nature*. 2008;453:662–666. doi: 10.1038/nature06892.
34. Atri D, Larrivee B, Eichmann A, Simons M. Endothelial signaling and the molecular basis of arteriovenous malformation. *Cell Mol Life Sci*. 2014;71:867–883.
35. Tillet E, Bailly S. Emerging roles of BMP9 and BMP10 in hereditary hemorrhagic telangiectasia. *Front Genet*. 2014;5:456. doi: 10.3389/fgene.2014.00456.
36. Lamouille S, Mallet C, Feige JJ, Bailly S. Activin receptor-like kinase 1 is implicated in the maturation phase of angiogenesis. *Blood*. 2002;100:4495–4501. doi: 10.1182/blood.V100.13.4495.
37. David L, Mallet C, Vailhé B, Lamouille S, Feige JJ, Bailly S. Activin receptor-like kinase 1 inhibits human microvascular endothelial cell migration: potential roles for JNK and ERK. *J Cell Physiol*. 2007;213:484–489. doi: 10.1002/jcp.21126.
38. Roman BL, Pham VN, Lawson ND, Kulik M, Childs S, Lekven AC, Garrity DM, Moon RT, Fishman MC, Lechleider RJ, Weinstein BM. Disruption of acvr1l1 increases endothelial cell number in zebrafish cranial vessels. *Development*. 2002;129:3009–3019.
39. Ricard N, Ciais D, Levet S, Subileau M, Mallet C, Zimmers TA, Lee SJ, Bidart M, Feige JJ, Bailly S. BMP9 and BMP10 are critical for postnatal retinal vascular remodeling. *Blood*. 2012;119:6162–6171. doi: 10.1182/blood-2012-01-407593.
40. Chen W, Sun Z, Han Z, Jun K, Camus M, Wankhede M, Mao L, Arnold T, Young WL, Su H. De novo cerebrovascular malformation in the adult mouse after endothelial Alk1 deletion and angiogenic stimulation. *Stroke*. 2014;45:900–902. doi: 10.1161/STROKEAHA.113.003655.
41. Baeyens N, Larrivee B, Ola R, Hayward-Piatkowski B, Dubrac A, Huang B, Ross TD, Coon BG, Min E, Tsarfati M, Tong H, Eichmann A, Schwartz MA. Defective fluid shear stress mechanotransduction mediates hereditary hemorrhagic telangiectasia. *J Cell Biol*. 2016;214:807–816. doi: 10.1083/jcb.201603106.
42. Ola R, Dubrac A, Han J, et al. PI3 kinase inhibition improves vascular malformations in mouse models of hereditary haemorrhagic telangiectasia. *Nat Commun*. 2016;7:13650. doi: 10.1038/ncomms13650.
43. Larrivee B, Prahst C, Gordon E, del Toro R, Mathivet T, Duarte A, Simons M, Eichmann A. ALK1 signaling inhibits angiogenesis by cooperating with the Notch pathway. *Dev Cell*. 2012;22:489–500. doi: 10.1016/j.devcel.2012.02.005.
44. Moya IM, Umans L, Maas E, Pereira PN, Beets K, Francis A, Sents W, Robertson EJ, Mummery CL, Huybredebroeck D, Zwijsen A. Stalk cell phenotype depends on integration of Notch and Smad1/5 signaling cascades. *Dev Cell*. 2012;22:501–514. doi: 10.1016/j.devcel.2012.01.007.
45. Aspalter IM, Gordon E, Dubrac A, Ragab A, Narloch J, Vizán P, Guedens I, Collins RT, Franco CA, Abrahams CL, Thurston G, Fruttiger M, Rosewell I, Eichmann A, Gerhardt H. Alk1 and Alk5 inhibition by Nrp1 controls vascular sprouting downstream of Notch. *Nat Commun*. 2015;6:7264. doi: 10.1038/ncomms8264.
46. Graupera M, Potente M. Regulation of angiogenesis by PI3K signaling networks. *Exp Cell Res*. 2013;319:1348–1355. doi: 10.1016/j.yexcr.2013.02.021.
47. Song MS, Salmena L, Pandolfi PP. The functions and regulation of the PTEN tumour suppressor. *Nat Rev Mol Cell Biol*. 2012;13:283–296. doi: 10.1038/nrm3330.
48. Worby CA, Dixon JE. PTEN. *Annu Rev Biochem*. 2014;83:641–669. doi: 10.1146/annurev-biochem-082411-113907.
49. Chamorro-Jorganes A, Lee MY, Araldi E, Landskroner-Eiger S, Fernández-Fuertes M, Sahraei M, Quiles Del Rey M, van Solingen C, Yu J, Fernández-Hernando C, Sessa WC, Suárez Y. VEGF-induced expression of miR-17-92 cluster in endothelial cells is mediated by ERK/ELK1 activation and regulates angiogenesis. *Circ Res*. 2016;118:38–47. doi: 10.1161/CIRCRESAHA.115.307408.
50. Hashimoto T, Mesa-Tejada R, Quick CM, Bollen AW, Joshi S, Pile-Spellman J, Lawton MT, Young WL. Evidence of increased endothelial cell turnover in brain arteriovenous malformations. *Neurosurgery*. 2001;49:124–131; discussion 131.
51. Du R, Hashimoto T, Tihan T, Young WL, Perry V, Lawton MT. Growth and regression of arteriovenous malformations in a patient with hereditary hemorrhagic telangiectasia. Case report. *J Neurosurg*. 2007;106:470–477. doi: 10.3171/jns.2007.106.3.470.
52. Hao Q, Zhu Y, Su H, Shen F, Yang GY, Kim H, Young WL. VEGF induces more severe cerebrovascular dysplasia in endoglin than in Alk1 mice. *Transl Stroke Res*. 2010;1:197–201. doi: 10.1007/s12975-010-0020-x.
53. Han C, Choe SW, Kim YH, Acharya AP, Keselowsky BG, Sorg BS, Lee YJ, Oh SP. VEGF neutralization can prevent and normalize arteriovenous malformations in an animal model for hereditary hemorrhagic telangiectasia 2. *Angiogenesis*. 2014;17:823–830. doi: 10.1007/s10456-014-9436-3.
54. Castel P, Carmona FJ, Grego-Bessa J, Berger MF, Viale A, Anderson KV, Bague S, Scaltriti M, Antonescu CR, Baselga E, Baselga J. Somatic PIK3CA mutations as a driver of sporadic venous malformations. *Sci Transl Med*. 2016;8:332ra42. doi: 10.1126/scitranslmed.aaf1164.
55. Geisthoff UW, Nguyen HL, Hess D. Improvement in hereditary hemorrhagic telangiectasia after treatment with the phosphoinositide 3-kinase inhibitor BKM120. *Ann Hematol*. 2014;93:703–704. doi: 10.1007/s00277-013-1845-7.

Highlights

- ALK1 (activin-receptor like kinase 1) negatively regulates endothelial cell proliferation by repressing PI3K (phosphatidylinositol 3-kinase) signaling through PTEN (phosphatase and tensin homolog) activation.
- Loss of ALK1 function in endothelial cells of patients with hereditary hemorrhagic telangiectasia 2 results in increased activation of PI3K signaling, enhanced endothelial cell proliferation, and in turn, vascular hyperplasia.
- We have also found a correlation between PI3K-activated vessels in the telangiectasias and the severity of epistaxis.
- Genetic or pharmacological inhibition of PI3K is sufficient to abolish the vascular hyperplasia induced by heterozygous loss of ALK1 in mouse retinas, providing the proof of concept for therapeutic intervention with PI3K inhibitors for the treatment of hereditary hemorrhagic telangiectasia.

Arteriosclerosis, Thrombosis, and Vascular Biology



JOURNAL OF THE AMERICAN HEART ASSOCIATION

ALK1 (Activin-Receptor Like Kinase 1) Loss Results in Vascular Hyperplasia in Mice and Humans Through PI3K (Phosphatidylinositol 3-Kinase) Activation

Elisenda Alsina-Sanchís, Yaiza García-Ibáñez, Ana M. Figueiredo, Carla Riera-Domingo, Agnès Figueras, Xavier Matias-Guiu, Oriol Casanovas, Luisa M. Botella, Miquel A. Pujana, Antoni Riera-Mestre, Mariona Graupera and Francesc Viñals

Arterioscler Thromb Vasc Biol. published online February 15, 2018;
Arteriosclerosis, Thrombosis, and Vascular Biology is published by the American Heart Association, 7272
Greenville Avenue, Dallas, TX 75231

Copyright © 2018 American Heart Association, Inc. All rights reserved.
Print ISSN: 1079-5642. Online ISSN: 1524-4636

The online version of this article, along with updated information and services, is located on the
World Wide Web at:

<http://atvb.ahajournals.org/content/early/2018/02/14/ATVBAHA.118.310760>

Data Supplement (unedited) at:

<http://atvb.ahajournals.org/content/suppl/2018/02/13/ATVBAHA.118.310760.DC1>

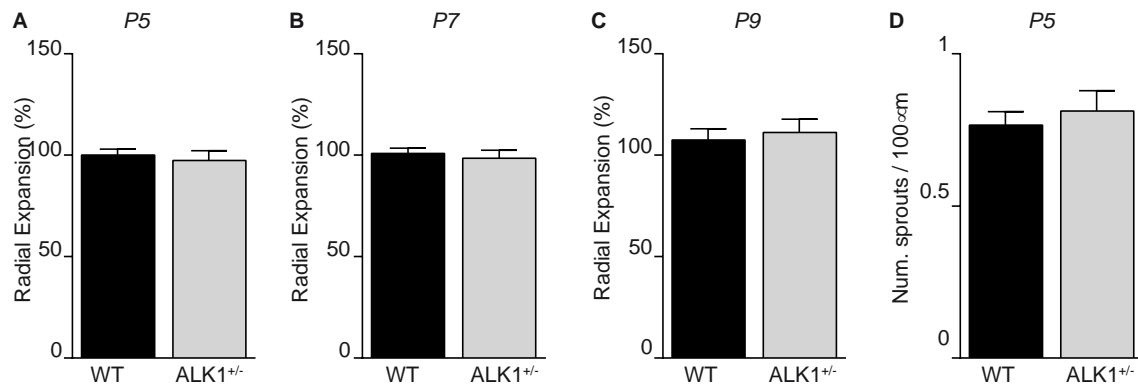
Permissions: Requests for permissions to reproduce figures, tables, or portions of articles originally published in *Arteriosclerosis, Thrombosis, and Vascular Biology* can be obtained via RightsLink, a service of the Copyright Clearance Center, not the Editorial Office. Once the online version of the published article for which permission is being requested is located, click Request Permissions in the middle column of the Web page under Services. Further information about this process is available in the [Permissions and Rights Question and Answer](#) document.

Reprints: Information about reprints can be found online at:
<http://www.lww.com/reprints>

Subscriptions: Information about subscribing to *Arteriosclerosis, Thrombosis, and Vascular Biology* is online at:
<http://atvb.ahajournals.org/subscriptions/>

SUPPLEMENTARY FIGURES AND TABLES

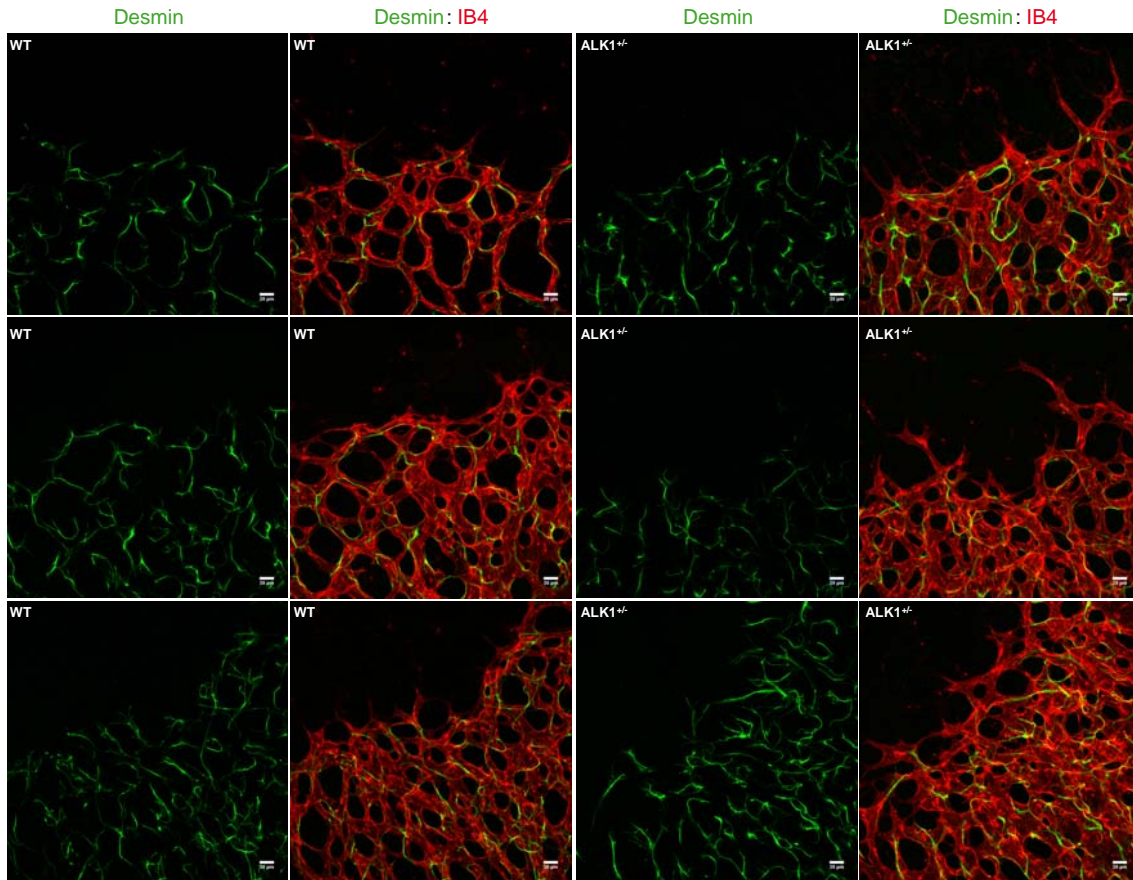
Supplementary Figure I



Supplementary Figure I: Retinal angiogenesis upon genetic inhibition of ALK1.

Quantification of radial vascular expansion of P5 (A), P7 (B) and P9 (C) retinas from wild type (WT) (n=8) or *ALK1*^{+/-} (n≥7) animals. (D) Quantification of sprouts number (tip cells) of P5 retinas from WT (n=12) or *ALK1*^{+/-} (n=15) animals. Error bars are standard error of the mean.

Supplementary Figure II

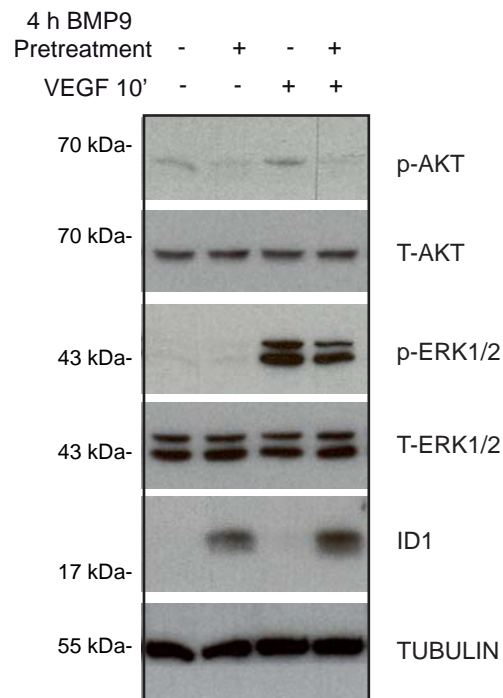


Supplementary Figure II: Heterozygous *ALK1* retinas show normal pericyte coverage.

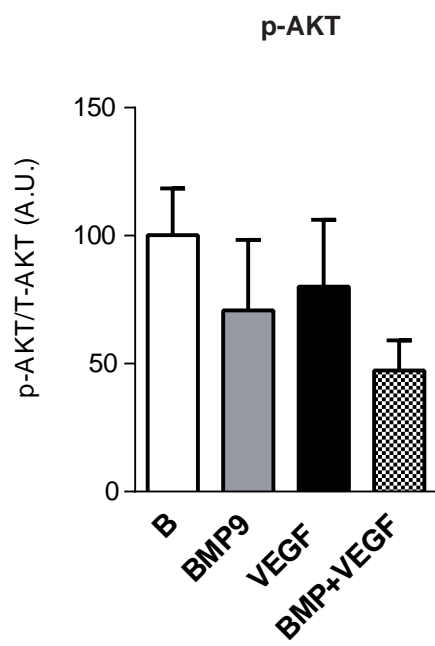
Whole-mount visualization of blood vessels by isolectin B4 (red) and pericytes (desmin staining, green) of P7 retinas from wild type (WT) or *ALK1*^{+/-} animals. We show images from three independent WT or *ALK1*^{+/-} animals.

Supplementary Figure III

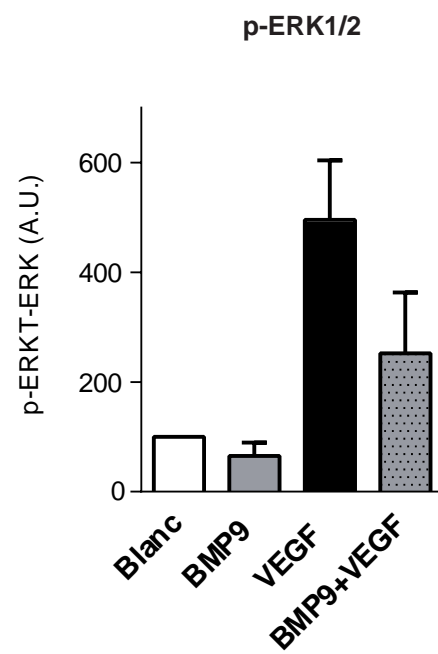
A



B

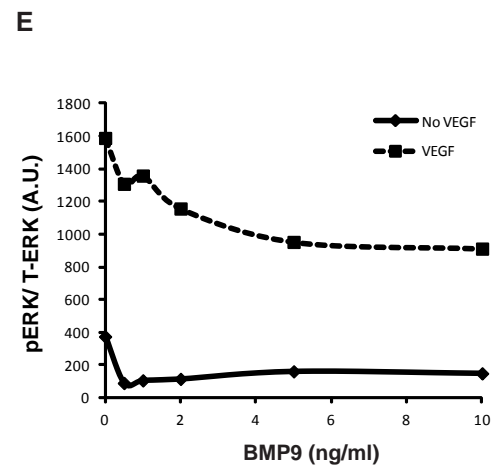
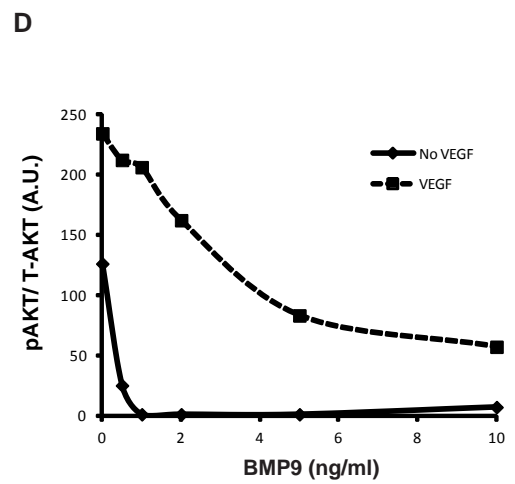
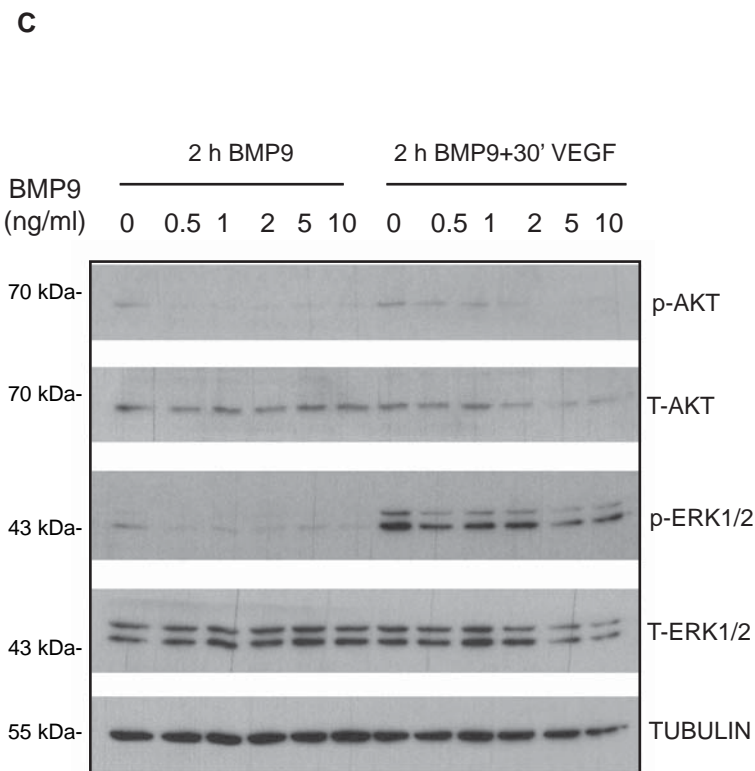
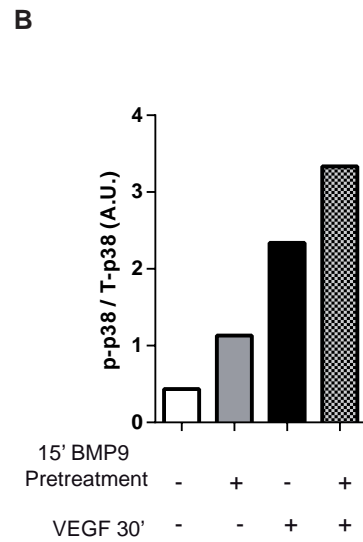
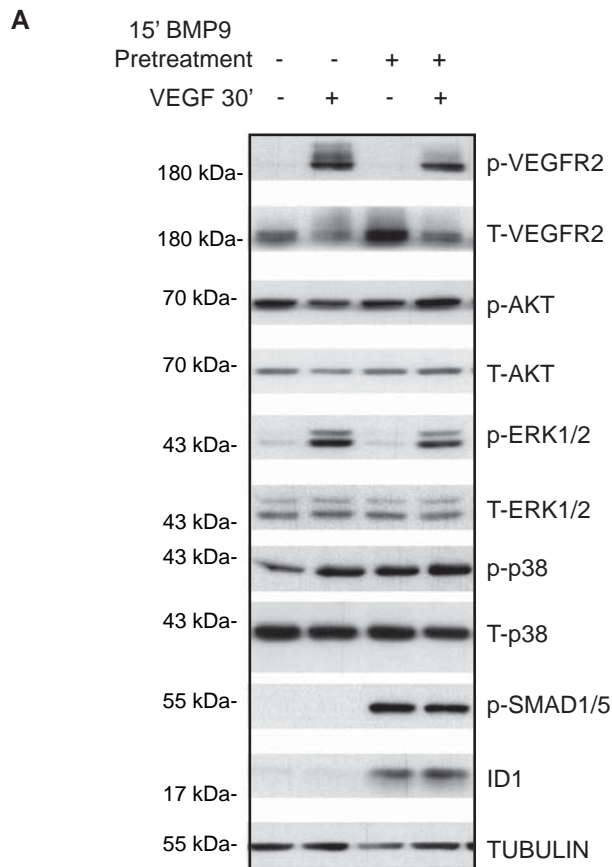


C



Supplementary Figure III: BMP9 blocks 10 min VEGF-induced AKT and ERK phosphorylation. (A) Growth factor-depleted HUVECs were pretreated or not with 10 ng/ml BMP9 for 4 h, then stimulated for an additional 10 min in the absence or presence of 10 ng/ml VEGF. Cells were lysed, and immunoblotted for the indicated antibodies. A representative blot from three independent experiments is shown. (B) Bars show quantification of the relative immunoreactivity of phosphoAKT (Ser473) normalized with respect to total AKT assessed as the mean of three independent experiments. (C) Bars show quantification of the relative immunoreactivity of phosphoERK1/2 normalized with respect to total ERK1/2. The mean of three independent experiments is shown. Error bars indicate the standard errors of the mean.

Supplementary Figure IV

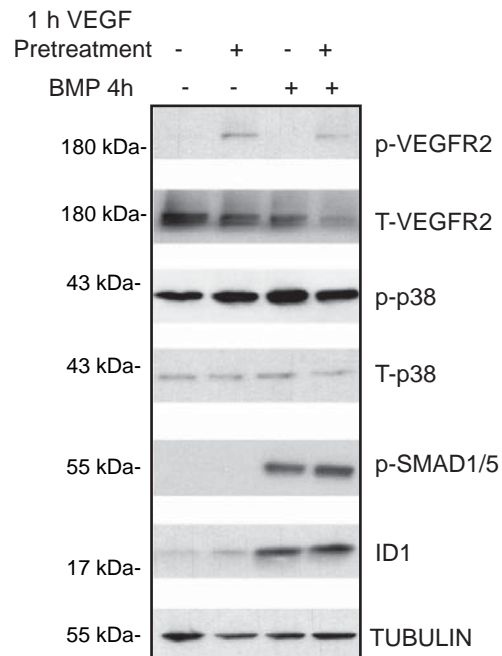


Supplementary Figure IV. Dose-response of BMP9

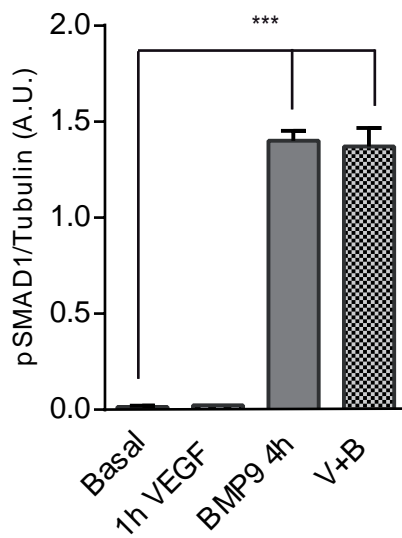
(A) Growth factor-depleted HUVECs were pretreated or not with 10 ng/ml BMP9 for 15 min, then stimulated for an additional 30 min in the absence or presence of 10 ng/ml VEGF. Cells were lysed, and immunoblotted for the indicated antibodies. A representative blot from two independent experiments is shown. (B) Bars show quantification of the relative immunoreactivity of phospho-p38 MAPK normalized with respect to total p38 MAPK assessed as the mean of two independent experiments. (C) Growth factor-depleted HUVECs were pretreated or not with 0, 0.5, 1, 2, 5 or 10 ng/ml BMP9 for 2 h, then stimulated for an additional 30 min in the absence or presence of 10 ng/ml VEGF. Cells were lysed, and immunoblotted for the indicated antibodies. A representative blot from two independent experiments is shown. (D) Bars show quantification of the relative immunoreactivity of phosphoAKT (Ser473) normalized with respect to total AKT assessed as the mean of two independent experiments. (E) Bars show quantification of the relative immunoreactivity of phosphoERK1/2 normalized with respect to total ERK1/2. The mean of two independent experiments is shown.

Supplementary Figure V

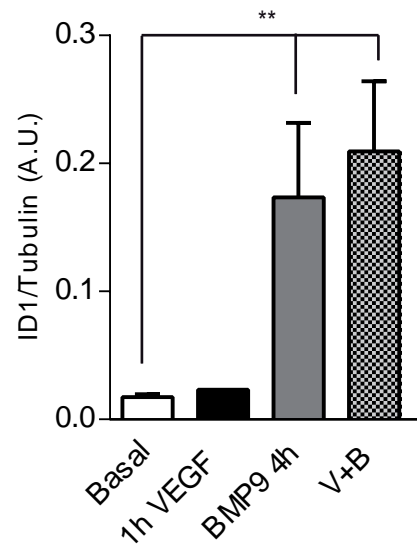
A



B



C

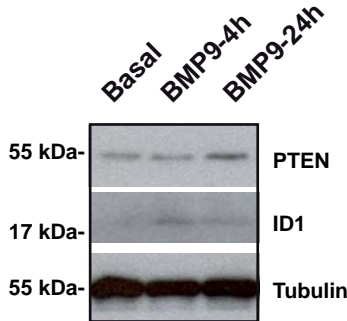


Supplementary Figure V: VEGF preincubation does not affect BMP9 signaling. (A)

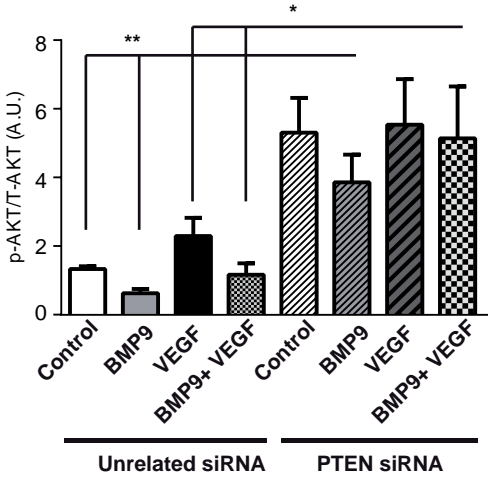
Growth factor-depleted HUVECs were pretreated or not with 10 ng/ml VEGF for 1 h, then stimulated for an additional 4 h in the absence or presence of 10 ng/ml BMP9. Cells were lysed, and immunoblotted for the indicated antibodies. A representative blot from three independent experiments is shown. **(B)** Bars show quantification of the relative immunoreactivity of phosphoSMAD1/5 normalized with respect to tubulin assessed as the mean of four independent experiments. **(C)** Bars show quantification of the relative immunoreactivity of ID1 normalized with respect to tubulin. The mean of four independent experiments is shown. Error bars indicate the standard errors of the mean. Statistical significance of two-tailed Mann-Whitney U tests: **, $p < 0.01$; ***, $p < 0.001$.

Supplementary Figure VI

A



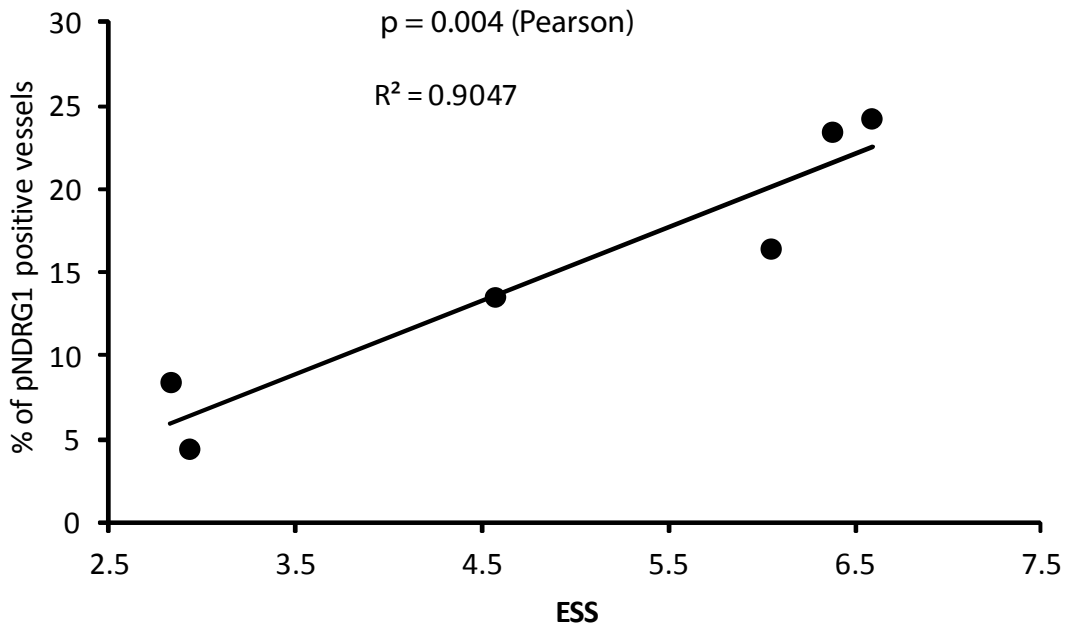
B



Supplementary Figure VI: Effect of BMP9 on PTEN expression

(A) Growth factor-depleted HUVECs were treated with vehicle or 10 ng/ml BMP9 for 4 or 24 h and immunoblotted using the indicated antibodies. A representative blot is shown of at least 5 independent experiments. (B) Bars show quantification of the relative immunoreactivity of phosphoAKT normalized with respect to total AKT assessed as the mean of five independent experiments. Error bars indicate the standard errors of the mean. Statistical significance of two-tailed Mann-Whitney U tests: *, $p < 0.05$; **, $p < 0.01$.

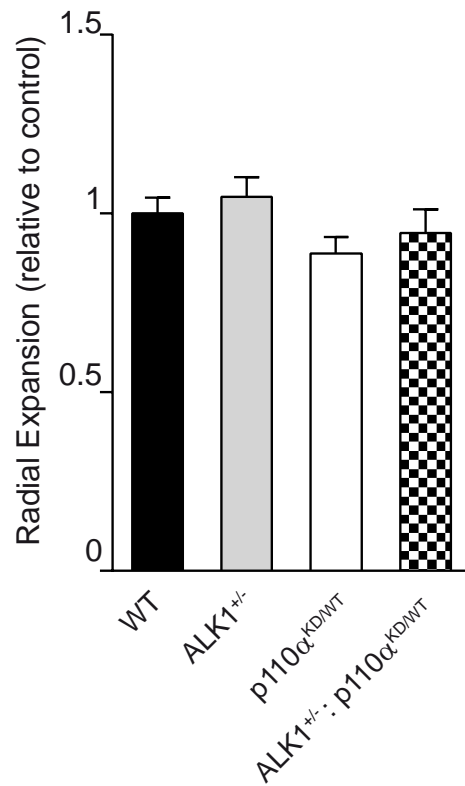
Supplementary Figure VII



Supplementary Figure VII: Positive correlation between pNDRG1 and nosebleed severity.

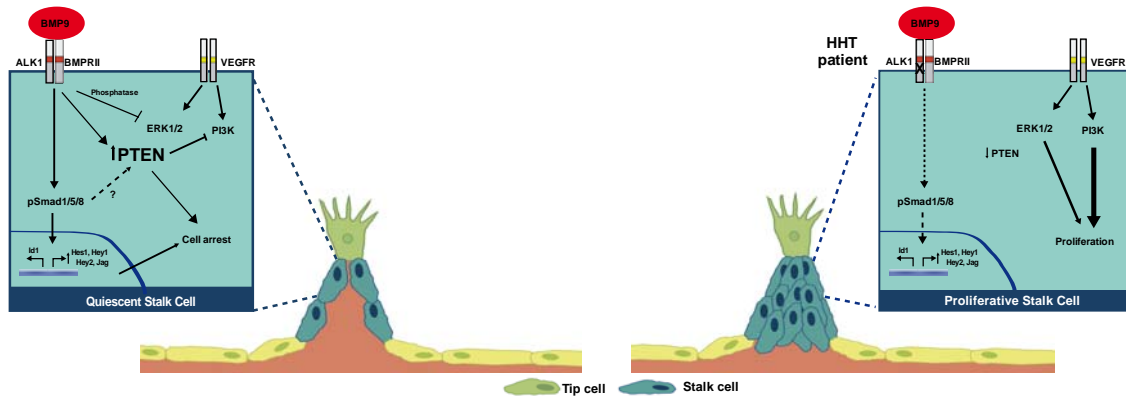
Correlation between grade of positivity for pNDRG1 and nosebleed severity measured by the Epistaxis Severity Score (ESS) in HHT2 patients analyzed in Fig. 5B and 5D. The two-tailed Pearson correlation coefficient is shown.

Supplementary Figure VIII



Supplementary Figure VIII: p110α regulates endothelial cell migration independently of ALK1. Quantification of radial expansion on P7 retinas from wild type (WT, n=4), *ALK1*^{+/-} (n=8), *p110α*^{KD/WT} (n=4) and *ALK1*^{+/-}/*p110α*^{KD/WT} (n=6) animals. Error bars are standard error of the mean.

Supplementary Figure IX



Supplementary Figure IX. Schematic model of BMP9 mechanistic effects in endothelial cells. Activation of ALK1 by BMP9 stimulates expression of PTEN, which in turn inhibits the PI3K signaling pathways and blocks stalk cell proliferation. Upon loss of ALK1 expression, such as in HHT2 patients, PTEN expression and activity are not stimulated, resulting in the overactivation of PI3K signaling and aberrant expansion of stalk cells.

Supplementary Table I. GSEA result of "Hallmark PI3K-AKT-MTOR signaling" in the comparison of telangiectasial and normal nasal tissue of HHT2 patients.

Gene symbol	Rank position	Running enrichment score	Contribution to association
<i>NFKB1B</i>	160	0,0203	Yes
<i>MAP2K6</i>	177	0,0468	Yes
<i>IRAK4</i>	197	0,0727	Yes
<i>EIF4E</i>	219	0,0979	Yes
<i>PTPN11</i>	330	0,1176	Yes
<i>CDK1</i>	540	0,1308	Yes
<i>SFN</i>	679	0,1461	Yes
<i>HRAS</i>	740	0,1645	Yes
<i>TIAM1</i>	959	0,1747	Yes
<i>MAPK1</i>	1015	0,192	Yes
<i>RPS6KA3</i>	1031	0,2111	Yes
<i>CDKN1A</i>	1195	0,2226	Yes
<i>PFN1</i>	1390	0,232	Yes
<i>GSK3B</i>	1677	0,2361	Yes
<i>NCK1</i>	1955	0,2399	Yes
<i>CDK2</i>	2462	0,2318	Yes
<i>MYD88</i>	2548	0,2426	Yes
<i>UBE2D3</i>	2689	0,2505	Yes
<i>RPS6KA1</i>	3055	0,2473	Yes
<i>GNGT1</i>	3095	0,2588	Yes
<i>MKNK1</i>	3291	0,2628	Yes
<i>ACTR3</i>	3363	0,2723	Yes
<i>PIKFYVE</i>	3387	0,2839	Yes
<i>SLC2A1</i>	3438	0,2941	Yes
<i>PPP1CA</i>	3447	0,3062	Yes
<i>TBK1</i>	3453	0,3184	Yes
<i>MAP2K3</i>	3523	0,3276	Yes
<i>ADCY2</i>	3576	0,3374	Yes
<i>PTEN</i>	3595	0,3487	Yes
<i>RIT1</i>	3685	0,3567	Yes
<i>TRAF2</i>	3849	0,3609	Yes
<i>TNFRSF1A</i>	3853	0,3724	Yes
<i>AKT1S1</i>	3874	0,3831	Yes
<i>MAPK8</i>	3890	0,394	Yes
<i>GRB2</i>	3926	0,404	Yes
<i>SQSTM1</i>	4088	0,4078	Yes
<i>PRKCB</i>	4112	0,4179	Yes
<i>CXCR4</i>	4645	0,404	Yes

<i>ACTR2</i>	4673	0,4129	Yes
<i>CFL1</i>	5025	0,4066	Yes
<i>RAF1</i>	5078	0,4136	Yes
<i>IL2RG</i>	5089	0,4226	Yes
<i>ARHGDI2A</i>	5148	0,4292	Yes
<i>DDIT3</i>	5208	0,4357	Yes
<i>VAV3</i>	5264	0,4423	Yes
<i>RAC1</i>	5608	0,4353	Yes
<i>PRKAG1</i>	5702	0,4394	Yes
<i>RALB</i>	5706	0,4477	Yes
<i>SLA</i>	5889	0,4475	Yes
<i>YWHAB</i>	5923	0,454	Yes
<i>PLCG1</i>	5960	0,4603	Yes
<i>CALR</i>	6436	0,446	Yes
<i>PITX2</i>	6525	0,4491	Yes
<i>THEM4</i>	6534	0,4558	Yes
<i>E2F1</i>	6586	0,4605	Yes
<i>CAB39</i>	6606	0,4666	Yes
<i>FGF22</i>	6695	0,4694	Yes
<i>DAPP1</i>	7241	0,4508	No
<i>ARF1</i>	7344	0,452	No
<i>MAPK10</i>	7897	0,432	No
<i>AP2M1</i>	8170	0,4243	No
<i>ARPC3</i>	8257	0,4249	No
<i>ACACA</i>	8361	0,4246	No
<i>PIK3R3</i>	8395	0,4274	No
<i>NOD1</i>	8596	0,4224	No
<i>UBE2N</i>	9365	0,3907	No
<i>CSNK2B</i>	9417	0,3913	No
<i>TRIB3</i>	9549	0,3881	No
<i>MAP3K7</i>	9608	0,3881	No
<i>CLTC</i>	9657	0,3885	No
<i>LCK</i>	10030	0,3738	No
<i>CDKN1B</i>	10147	0,3706	No
<i>EGFR</i>	10171	0,3714	No
<i>AKT1</i>	10339	0,3656	No
<i>ATF1</i>	10433	0,3629	No
<i>PIN1</i>	11043	0,3362	No
<i>PLA2G12A</i>	11074	0,3356	No
<i>CAB39L</i>	11279	0,3268	No
<i>PRKAR2A</i>	12228	0,2847	No
<i>SMAD2</i>	12305	0,282	No
<i>MAPKAP1</i>	12891	0,2572	No

<i>PPP2R1B</i>	13085	0,2503	No
<i>RIPK1</i>	13251	0,2449	No
<i>RPTOR</i>	13459	0,2378	No
<i>NGF</i>	13718	0,2288	No
<i>DUSP3</i>	14234	0,2088	No
<i>HSP90B1</i>	15052	0,1762	No
<i>ADRBK1</i>	15806	0,1474	No
<i>MAPK9</i>	15862	0,1503	No
<i>MKNK2</i>	16266	0,1379	No
<i>CDK4</i>	16270	0,1436	No
<i>TSC2</i>	16315	0,1475	No
<i>FASLG</i>	16394	0,1501	No
<i>PRKAA2</i>	16473	0,1527	No
<i>IL4</i>	16528	0,1565	No
<i>CAMK4</i>	17734	0,11	No
<i>GNAI4</i>	17897	0,1109	No
<i>ITPR2</i>	17932	0,1177	No
<i>PDK1</i>	18067	0,1202	No
<i>FGF6</i>	18290	0,1191	No
<i>PAK4</i>	18642	0,1127	No
<i>STAT2</i>	19127	0,1013	No
<i>PLCB1</i>	19834	0,0814	No
<i>ECSIT</i>	19920	0,0897	No
<i>FGF17</i>	20747	0,0669	No